Turkish Journal of Engineering
https://dergipark.org.tr/en/pub/tuje
e-ISSN 2587-1366

Uranium migration and radioactive characteristics of the Sarıçiçek and Sarıhan Granodiorites

Suna Altundaş *[1], **Hakan Çınar** [2]

[1]Gümüşhane University, Faculty of Engineering and Natural Sciences, Department of Geophysics Engineering, Türkiye
[2]Karadeniz Technical University, Faculty of Engineering, Department of Geophysics Engineering, Türkiye

Keywords
Gamma-Ray Spectrometer
Radioelement Composition
F Parameter
Radioelement Ratios
Uranium Migration

Research Article
DOI: 10.31127/tuje.1100375

Received: 08.04.2022
Accepted: 07.07.2022
Published: 31.08.2022

Abstract

The radionuclide concentrations of eU (ppm), eTh (ppm), K (%) and dose rate values were measured in Sarıçiçek (Gümüşhane) and Sarıhan (Bayburt) granodiorites for a duration of 5 minutes at each of 532 measurement points. The radioelement ratios (eU/eTh, eU/K, and eTh/K) indicating the origins of the rocks, the geochemical indicators (U_{me}, F parameter, and eU-(eTh/3,5) rate) showing the uranium mobility and the radioelement concentrations were calculated and mapped within the study areas. The average K, eU, and eTh concentrations were calculated as 2.98%, 3.15 ppm, and 12.45 ppm for Sarıçiçek granodiorite, and 1.83%, 2.73 ppm, and 13.6 ppm for Sarıhan granodiorite, respectively. Higher radioactivity values were observed in basaltic, sedimentary, and ultramafic rock combinations within the granodiorite masses. In the classification according to radioelement ratios, it was concluded that the rocks in the study areas formed as a mixture of upper mantle and crustal materials. In both study areas, there was uranium transport from the granodioritic masses into the surrounding rocks, and accordingly, the rocks in the surrounding formations were enriched in uranium. As a result, radioactivity levels, rock formation origins, and uranium transport of both granodioritic masses and rocks in the surrounding formations were determined by evaluation with radioelement concentration values and ratios and migration parameters. The study areas were characterized by associating them with geology in light of radioactive data.

1. Introduction

The natural radioactivity existing on earth has affected all living things directly or indirectly since the formation of the earth. This natural radioactivity includes cosmic rays coming from outer space especially, and the rays emitted as a result of the decay of natural radionuclides in rocks, soil, water, and even the air we breathe. The natural radioactivity level of a place varies depending on the geological structure, geographical location, and radiochemical characteristics of the region. Factors such as rain, snow, low pressure, high pressure, and wind direction also determine the magnitude of the natural radiation level. People are exposed to different types of radiation emitted from these sources in the natural environment in which they live. The most common natural radiation sources are ^{40}K, ^{238}U, ^{226}Ra, and ^{232}Th isotopes [1].

The amounts of these radionuclides, which contribute to environmental radioactivity, in nature may vary according to soil and rock types. Natural radioactivity in soils and rocks provides the largest contribution to the environmental gamma dose rate. For example, natural radioactivity in volcanic rocks is higher than in sedimentary rocks. The level of radioactivity in sedimentary and phosphate-type rocks is also quite high [2-3]. Granites are very common plutonic rocks in most of the earth. Granites gain prominence radiologically because they contain high proportions of ^{238}U, ^{232}Th, and ^{40}K. Granite rocks spread over large areas in many regions and contain significant levels of Th. As a result of radiometric studies carried out around the world and in Turkey, gamma radiation was measured in areas with very high radiation values [4].

Metamorphic rocks, granitic rocks, sediments containing organic matter, sandstones, and carbonate sedimentary rocks are rock groups rich in uranium, thorium, radium, and radon. The presence of uranium and thorium in igneous rocks is closely related to changes in uranium and thorium concentrations and igneous crystallization of magma. The uranium and

* **Corresponding Author**
*(sunaaltundas@gmail.com) ORCID ID 0000-0002-5840-0352
(cinar@ktu.edu.tr) ORCID ID 0000-0002-6562-1962

Cite this article
Altundaş, S., & Çınar, H. (2023). Uranium migration and radioactive characteristics of the Sarıçiçek and Sarıhan Granodiorites. Turkish Journal of Engineering, 7(3), 208-226

thorium content in igneous rocks decreases from acidic rocks to basic rocks [5].

The natural radionuclides these rocks contain should be determined and examined radiologically, especially due to the use of granite as a building material inside and outside buildings. In terms of natural radioactivity, although the abundance of natural radioelements in the oceanic crust and the mantle is very low, the content of these elements in granitic rocks is very high. According to geologists, the cause of this is the fractional crystallization of magma and partial melting [6]. Especially high concentrations of radioactivity were detected in igneous rocks such as granite. Granite is distributed over large areas in many regions and contains significant amounts of thorium [7]. The eU (equivalent uranium)/eTh (equivalent thorium) ratio is highly affected by the oxidation process and this process causes uranium (U) migration. This ratio is a very important parameter in determining the oxidation area of U [8]. Since uranium is a mobile element, it can covert from U^{+4} to U^{+6} during oxidation. U can migrate from one place to another and react with the elements there. The eU/eTh ratio is a very important geochemical parameter for U migration.

Most of the earth-forming rocks, ground, and surficial waters containing these elements have radioactive properties. Both airborne and land-borne gamma-ray spectrometer studies are usually used for purposes such as uranium prospecting, surficial geological mapping, and soil mapping in agriculture, stratigraphic analyses of geological formations, geothermal research, and metallic mining research [9]. There are many scientific studies related to the definition of the natural radiation level in rock and soils [10-11], lithological discrimination-related studies [12-14], radionuclide concentrations in volcanic rocks and granitic plutons [15-19], radioactive areas of mineralization [20-22], possible uranium migration areas and the migration paths in granitic rock [23-27].

In this study, the Sarıçiçek granodiorite (Gümüşhane) and Sarıhan granodiorite and surrounding formations (Bayburt) containing different lithological units located in the Eastern Pontides, Turkey was selected as the study areas. Sarıçiçek granodiorite, surrounded by Early Eocene volcanic rocks of the Alibaba Formation, is part of the composite E–W-trending Kaçkar Batholith in the Eastern Pontides of Eastern Turkey. The rocks outcropping in the Sarıçiçek granodiorite are I-type granodiorite rocks and generally change from calc-alkaline composition to high K calc-alkaline composition [28]. Sarıhan granodiorite and its surrounding formations located in the Eastern Pontides, Turkey comprises three different lithological units namely, Hozbirikyayla Formation (limestone and sandy limestones), Sarıhan granodiorite (consisting of quartz monzodiorite, granodiorite, and quartz diorite), and ophiolitic mélange (andesite, basalt, sandstone, gravelly sandstone) [29]. The pluton has calc-alkaline composition and is characterized by a calc-alkaline granodiorite trend [30].

Within the scope of this study, concentrations of equivalent uranium (eU, in ppm), equivalent thorium (eTh, in ppm), potassium (K, in %) and dose rate values of the Sarıçiçek (Gümüşhane) and Sarıhan granodiorites (Bayburt) and surrounding formations were investigated using the gamma-ray spectrometry method. An attempt was made to correlate the obtained radionuclide concentration changes with the geology of the study areas. Using the radionuclide concentrations obtained from measurements made in the field, the geochemical element ratios provide information about the origin of the rocks and the migration tendency of the natural radionuclides in the rocks, especially U, was calculated and mapped.

2. Location and geological background of the study areas

2.1. General setting of the study areas

Within the scope of this study, radioactivity measurements were carried out in and around the Sarıçiçek granodiorite (Gümüşhane) located between 40º 25' 30.61'' and 40º 26' 33.94'' north latitude and 39º 49' 28.70'' and 39º 52' 3.69'' east longitude and in Sarıhan granodiorite and its surroundings (Bayburt), which is located between 40º 04' 56.03'' northern latitude and 39º 57' 28.81'' and 40º 08' 56.87'' east longitude (Fig. 1).

The Sarıçiçek granodiorite is located approximately 30 km west of Gümüşhane city (between map sheets H43 b1-b2), southeast of the Eastern Black Sea Mountains (Pontides). The Sarıçiçek granodiorite has an ellipsoidal shape and is approximately 7x2.3 km in size. The long axis of the granodiorite is in the NE-SW direction. Sarıhan granodiorite is approximately 40 km south of Bayburt and on map sheets Trabzon H44 d1-d4. While most of the study area is within the borders of the province of Bayburt, part of the mélange belt is within the borders of the province of Erzincan. This pluton crops out in an area of approximately 40 km^2.

2.2. Geological Structure

The Pontide Orogenic Belt constitutes an essential part of the Alpine-Himalayan system and geographically corresponds to the Black Sea and Thrace regions in Turkey [31]. The Eastern Pontide Orogenic Belt (Fig. 2), which includes the study areas, was divided into three subunits as north, south, and axis zones from north to south by considering different lithological features and facies changes [32-33].

In the northern zone, in general, Late Mesozoic and Cenozoic granitic rocks and volcanic rocks constitute the dominant lithology. Moving south, the igneous rock-dominated sequence in the north is replaced by a sequence dominated by sedimentary rocks.

In the axis zone, the serpentinized ultramafic masses and Miocene volcanic-sedimentary rocks are the dominant rock lithologies [34]. The areas investigated within the scope of the study crop out in the southern zone of the Eastern Pontide Orogenic Belt (Fig. 3a).

Sarıçiçek granodiorite (Fig. 3b), which is the second of the studied masses and crops out approximately 30 km west of Gümüşhane city center, close to the northern part of the southern zone, is surrounded by Eocene volcanic rocks [36].

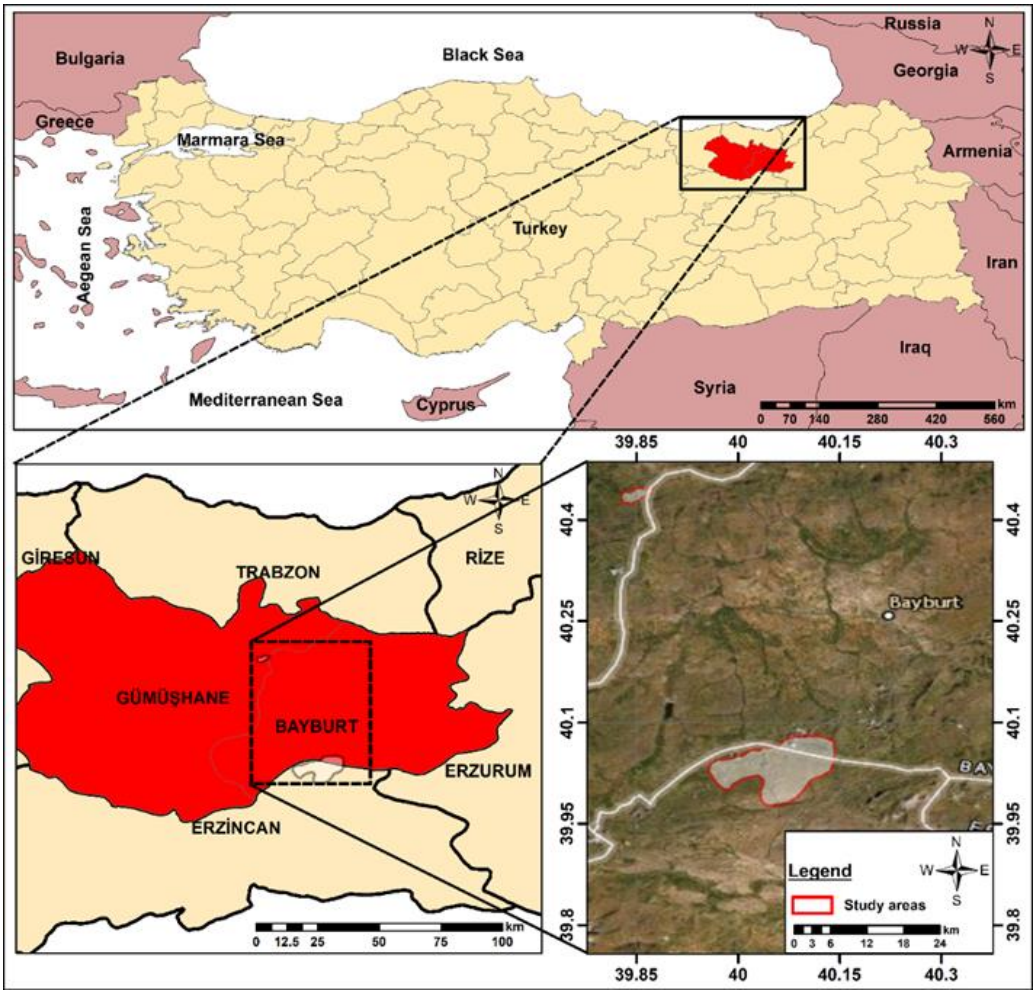

Figure 1. Location map of the studied areas in the Gümüşhane (Sarıçiçek) and Bayburt (Sarıhan)

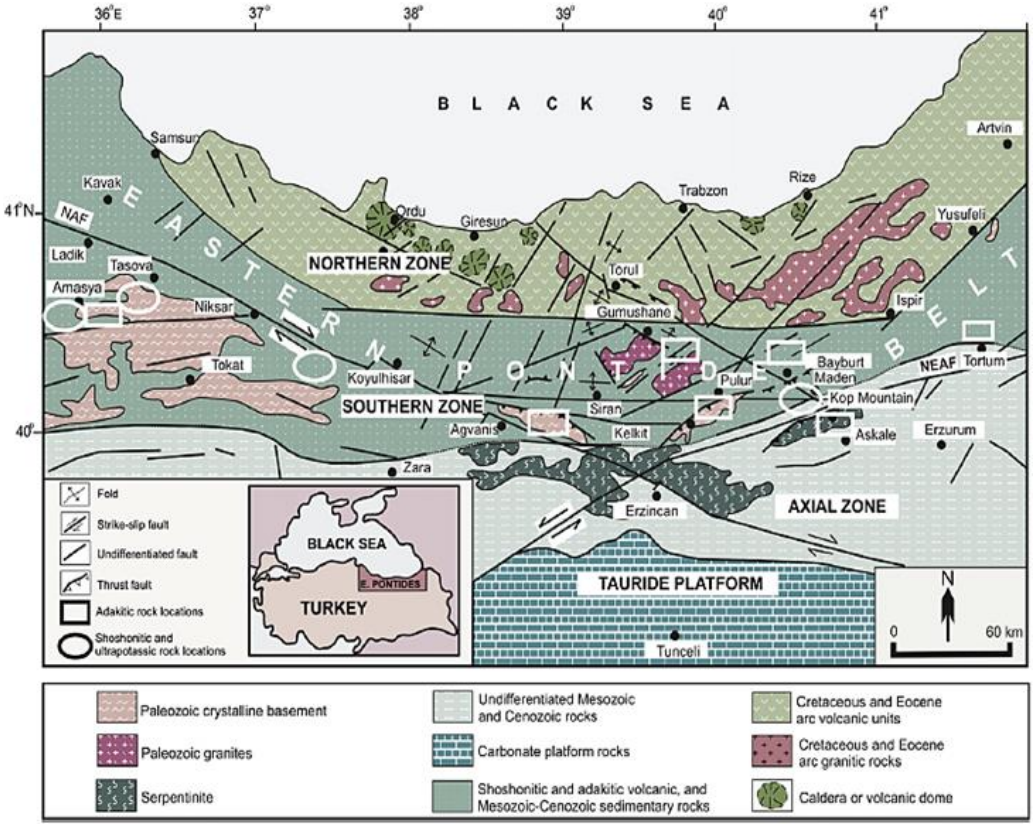

Figure 2. Main tectonic features and zones of the eastern Pontides orogenic belt (NAF: North Anatolian Fault; NEAF: Northeast Anatolian Fault) modified from [35]

In this area, which reflects the typical features of the southern zone, the Eocene Alibaba Formation is represented by a thick volcanic and pyroclastic sequence that developed following the deposition of nummulitic limestones overlying a conglomeratic level at the base. Compared to the Sarıhan granodiorite in the south, it contains fewer enclaves, and plagioclase, amphibole, and biotite crystals can be observed macroscopically on hand samples from the rocks forming this mass. The rocks outcropping in Sarıçiçek granodiorite (Fig. 3b) are I-type granodiorite rocks and generally change from calc-alkaline composition to high K calc-alkaline composition [28]. The age of the mass was determined as Lutetian as a result of Ar/Ar dating performed on mafic minerals [36] and U-Pb dating of zircons [37].

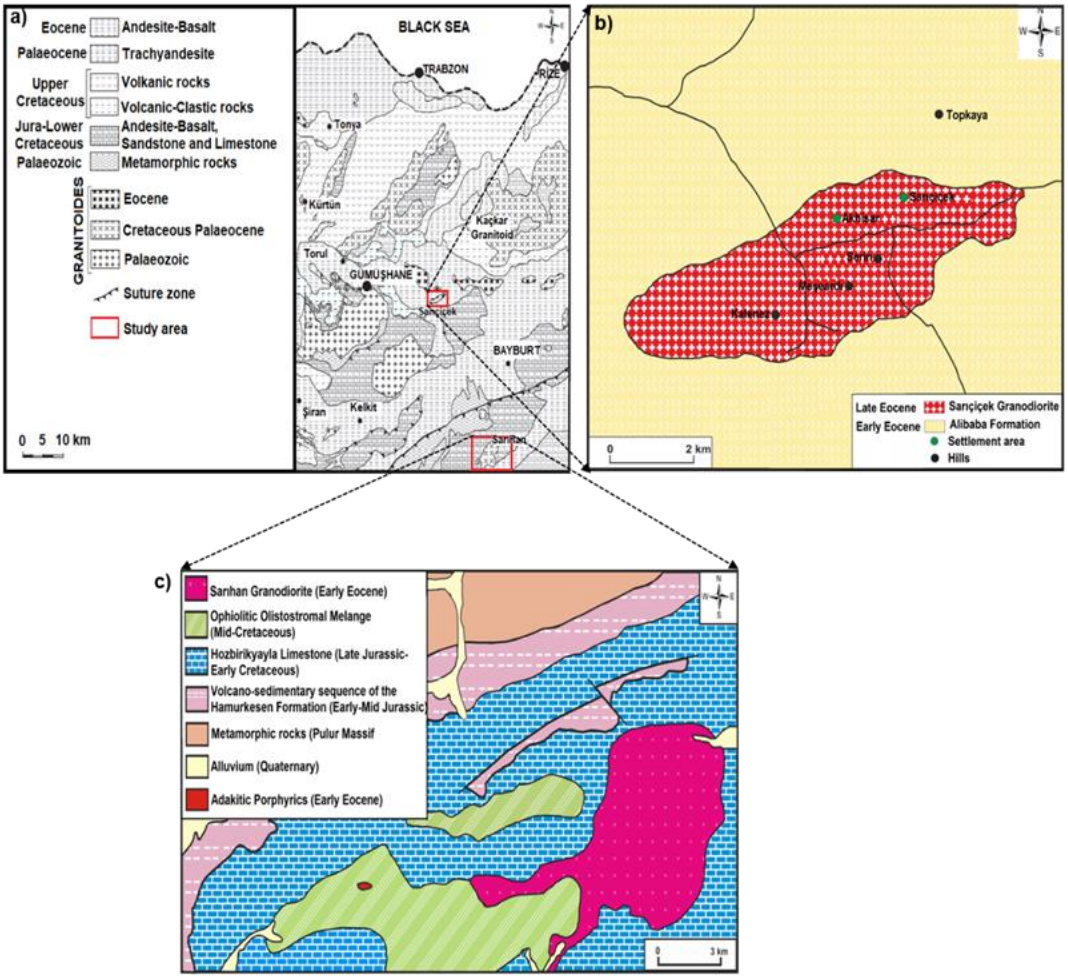

Figure 3. a) The geology map of the studied area modified from [38] b) The Sarıçiçek granodiorite and surroundings modified from [28] and c) The Sarıhan granodiorite and its relationship with the surroundings rocks modified from [30] and [39]

Sarıhan granodiorite (Fig. 3c), which is located in the southern zone and is further south compared to the first study area, is one of the largest intrusive masses with adakitic composition in the Eastern Pontides [39]. Sarıhan granodiorite has contacts with the Middle Cretaceous Otlukbeli mélange and the Late Jurassic-Early Cretaceous Hozbirikyayla Limestone. Traces of contact metamorphism and skarn mineralization are usual, especially along with the contact with limestones [30]. The mass, which presents a rather massive appearance, is characterized by well-developed and unfilled fracture systems. In addition, mafic microgranular enclaves are commonly seen in the mass, indicating magma mixture, and the diameters of the enclaves reach 40 cm in places (Fig. 4). In a study of felsic intrusions cropping out in the Pulur massif [38], zircons selected from the samples taken from this mass were aged by the U-Pb dating method, and Early Eocene age of approximately 53 million years was obtained. It was emphasized for the first time that this rock mass has adakitic composition. The Sarıhan granodiorite is a metalumin-based, calc-alkaline, and I-type granitoid [40].

Figure 4. Mafic microgranular enclave and Aplit dyke found in Sarıhan granodiorite

3. Material and Method

3.1. In-situ Gamma-Ray measurements

Gamma-ray spectrometry has been used for uranium exploration, geological mapping studies, and earthquake monitoring studies [9]. Since the existence of the universe, K, U, and Th radionuclides are found in greater or lesser amounts in rocks within a zone up to a depth of about 10-12 km within the earth's crust. The average concentrations of these elements in the earth's crust are 2.33 % for K, 3 ppm for U, and 12 ppm for Th [41]. The gamma-ray spectrometer used in the study was an instrument designed for natural and artificial radioisotope measurements on cores taken by drilling in the field and laboratories or on rock-soil samples collected from the field. Gamma rays emitted can be measured as a physical property because rocks contain different radioactive elements in different proportions and some minerals contain radioactive elements in different proportions. U, Th, and K elements and their isotopes, which have this radioactive feature and are found in significant proportions in the earth's crust, have great importance in geological and geophysical research. The isotopes of these elements emit gamma-rays at certain energy levels. With gamma-ray spectrometry, these gamma rays are measured in certain energy ranges. For this reason, gamma-ray spectrometry is an important radiometry technique applied in the investigation of many issues related to the earth. With radioactivity measurements made on soil or rocks, the number of radioactive elements by weight at each point (K (%), eTh (ppm), eU (ppm)) is measured. Determination of uranium and thorium is based on the assumption that the daughter elements are in equilibrium with the parent elements; that is, none of the steps in the decay series were disturbed. Based on this assumption, the amounts of uranium and thorium released are equivalent to the value in equilibrium with the measured radioactivity of the isotopes of thallium or bismuth. For this reason, gamma-ray measurement results are expressed as 'equivalent uranium (eU)' and 'equivalent thorium (eTh)'. There are three important gamma-ray energies from high to low: 2.62 MeV for thorium (^{208}Tl), 1.76 MeV (^{214}Bi) for uranium, and 1.46 MeV (^{40}K) for potassium [42-43].

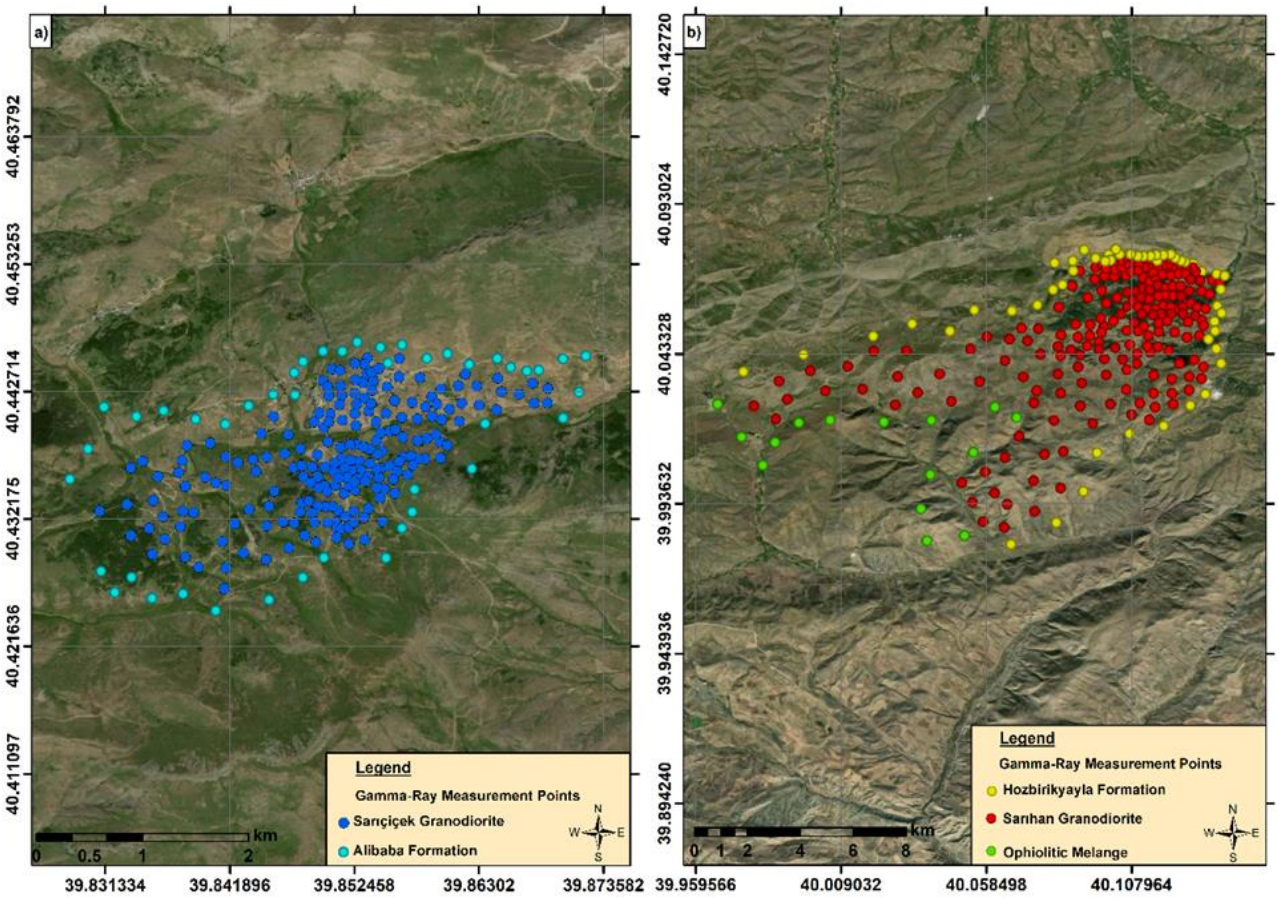

Figure 5. In-situ gamma-ray measurement points in the study areas

In-situ gamma-ray spectrometry measurements were made in and around Sarıçiçek and Sarıhan granodiorites at 532 points in total, forming an irregular grid owing to topographical difficulties. Of these, 265 points were measured on outcropping rock and soils in Sarıçiçek granodiorite and surrounding formations and 267 were measured on Sarıhan granodiorite and its surrounding formations (Fig. 5). The measurement time was set to 5 minutes for each point, and the coordinates of the points were recorded using a handheld GPS. In addition to radiometric parameters (K, eU, eTh, and dose rate) obtained from measurements in the field, the radionuclide ratios (eU/eTh, eU/K, and eTh/K) provide information about the origin of the rocks. Geochemical indicators (U_{me}, F parameter, and eU-(eTh/3,5) rate) showing uranium remobilization in the rocks and the

relationship between radioelement concentrations were calculated and these data were mapped. By evaluating the maps together, the presence of uranium migration can be assessed and the direction of possible uranium migration was determined in the study areas.

3.1.1. Natural radionuclide ratios (K/eTh, eU/eTh, and eU/K)

Some factors that affect radionuclide concentrations, such as soil moisture content, condition of outcropping rock, vegetation, and geometric structure of the land, have a lesser effect on these radionuclide ratios. The radionuclide ratios (K/eTh, eU/K, and eU/eTh) that provide information about the origins of rocks are frequently used in the detailed interpretation of in situ radioactivity measurements. For example, eU/K and eU/eTh ratios are particularly useful to reveal uranium-rich areas [44-45].

3.1.2. Geochemical indicators of uranium remobilization

Uranium, which is a mobile element, migrates from its source to another location. The expected original uranium content was calculated by dividing the eTh content (eTh/eU) ratio by the value (3.5) for granite to understand uranium remobilization in the region [46]. The result is the hypothetical uranium distribution. This helps define the trends of uranium migration. When the eU-(eTh/3.5) values are mapped, it is accepted that negative contour areas indicate uranium-poor areas, while the areas with positive contours show places where uranium enrichment occurs. By subtracting the original uranium content (U_0) from the available uranium content (U_p), the uranium migration value (U_m) for a particular rock can be estimated [47]. The original uranium content (U_0) can be calculated by multiplying the average thorium content by the average regional eU/eTh ratio in various lithological units (U_0=eTh×(regional eU/eTh)).

If the original uranium content (U_0) is known from the available uranium content (U_p) in soil and rocks, we can calculate the uranium migration rate (U_{me} %) using the following equation;

$$\%U_{me} = (U_m/U_p) \times 100 \quad (1)$$

U_{me} (%) values have two states; if Ume is >0, this indicates that uranium migration took place within the geological body. If U_{me} <0, it means that uranium migration did not occur within the geological body [48].

High degrees of uranium transfer in the rock is due to the high degree of correlation between eU and eU/eTh ratio. For additional information about the redistribution of radioactive elements, the inverse ratio between the eU/eTh ratio and the eTh content in different lithological units can be used. In deriving the degree of rock alteration, the F parameter was used [49]. The F parameter is given by the following equation:

$$F = K/(eTh/eU) = eU/(eTh/K) = K \times (eU/eTh) \quad (2)$$

Using this parameter, we can describe two specific characteristics of rock environments: one is the uranium abundance relative to eTh/K, and the other is the potassium abundance relative to eTh/eU. Therefore, the use of the F parameter is effective in identifying strong K-alteration zones associated with uranium mineralization [50].

3.2. Gamma-Ray measurements in the laboratory

Rock and soil samples were taken from the study areas to test the sensitivity of the spectrometer and the concentration difference that may occur depending on the detector used between measurements using field and laboratory environment (Fig. 6). Soil samples were taken from a depth of 30 cm from the surface by removing foreign objects such as stones, grass, wood chips, and tree bark. The rock samples were collected from the rock by cleaning the mossy and altered parts of the exposed rocks.

Figure 6. Soil and rock samples collected from the Sarıçiçek granodiorite and surroundings

All soil and rock samples taken from the field were left to dry in a laboratory environment for 15-20 days. The dried soil and the rock samples were crushed and after the necessary stages were passed through a 2 mm sieve to create homogeneous samples. Samples were placed into 100 ml plastic measuring cups with a diameter of 55 mm and a height of 65 mm, prepared for the experimental geometry, and kept for one month after the caps were tightly closed [15].

Figure 7. Canberra GC 1519 model HPGe detector

In the spectrometric analysis carried out in the laboratory, only 84 samples were used from the samples

collected from Sarıçiçek granodiorite and surroundings, due to the large number of samples collected. The measurement time was approximately one day. A Canberra, GC 1519 model HPGe detector, which has a resolution of 1.9 keV at 1332.5 keV gamma of ^{60}Co and relative efficiency of 15%, was used for radioactivity measurements of the samples (Fig. 7). Gamma spectrometry uses a detector, preamplifier, spectroscopy amplifier, analog-digital converter (ADC) system that converts analog counts into electronic signals, and multi-channel analyzer (MCA). The detector was shielded with cylindrical lead with a thickness 10 cm that contains an inner concentric cylinder of Cu with a thickness of 2 mm in order to reduce the background effects [5]. The sample counting time was determined as 80000 s. The obtained spectra were analyzed using the Genie-2000 program, and the activity concentrations were calculated.

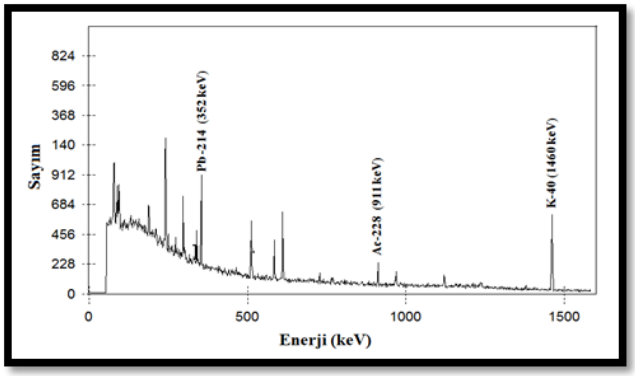

Figure 8. Gamma ray spectrum of a rock sample taken from Sarıçiçek granodiorite

In Fig. 8, the gamma ray spectrum is presented for one of the rock samples from the Sarıçiçek granodiorite measured with the HPGe detector. By using energy calibration, the energy values of the peaks and corresponding radioisotopes were determined. During the study, the energy calibration was checked periodically. Peaks for the decay products of ^{238}U (^{226}Ra (186.21 keV), ^{214}Pb (351.9 keV), ^{214}Bi (609.3 keV)) and ^{232}Th series (^{208}Tl (583.1 keV) and ^{228}Ac (911.1 keV)), ^{40}K (1460.8 keV) and ^{137}Cs (661.6 keV) were taken into account and the relevant area (ROI) regions were selected for each peak. In addition, the areas of the peaks were marked to give the largest area and the smallest error. Taking into account the detector efficiency, the specific activity concentration of these natural radionuclides, A (Bq.kg^{-1}) was calculated from the following equation.

$$C = \frac{N}{\varepsilon \times P_\gamma \times t \times m} \qquad (3)$$

N, ε, Pγ, t, and m in this formula represent the net counting rate (counts per second), the detector efficiency, the absolute transition probability of gamma-decay of the nuclide, the counting time (seconds), and mass of the sample in kg [5]. The net areas under the peaks were obtained by subtracting the background (peak areas from the blank measurement for each calculated element) from the total area.

4. Results and Discussion

4.1. Assessment of In-situ Gamma-ray Data in the Sarıçiçek Granodiorite and Surroundings

The natural radioactivity level of a region varies depending on both the radionuclide concentrations in the soil and rocks in the region and the distance of the area from the sea. While the altitude of the measurement area in Gümüşhane varied between 1900-2200 m, this value varied between 1800 m and 2300 m in the second study area of the Sarıhan granodiorite. This situation is one of the reasons for the high gamma dose ratio values in the regions. Since the altitude from the sea increases in direct proportion to the amount of cosmic radiation, the amount of gamma radiation also increases accordingly. When we examine the geological structure of the region, while Sarıçiçek granodiorite and its surroundings mainly consist of granite, granodiorite, quartz monzonite, and quartz monzodiorite composition rocks, this unit is surrounded by the Alibaba Formation and the rock types contain eU, eTh, and K which exist spontaneously in different proportions.

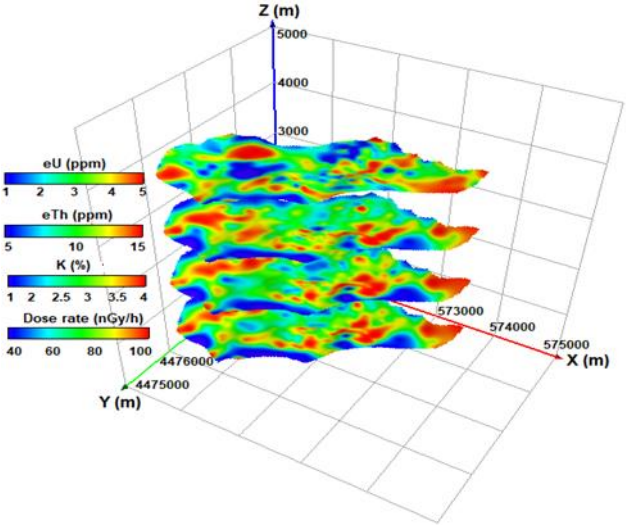

Figure 9. Three-dimensional representation of eU, eTh, K concentrations and dose rate distribution of Sarıçiçek granodiorite and surroundings (Gümüşhane) modified from [15].

The highest concentration and dose rate values (from orange to red) are seen for the Sarıçiçek granodiorite, while the lowest (from dark blue to light blue) values were obtained from the Alibaba Formation surrounding the plutonic mass (Fig. 9). Finally, the medium values defined by a color scale ranging from green to yellow are distributed in the whole area. While the highest concentrations of equivalent thorium, potassium, and dose rate values were recorded in the plutonic mass consisting of granite, granodiorite, quartz monzonite, and quartz monzodiorite composition rocks, the lowest equivalent uranium value was measured in this mass. The lowest concentration values were found in the Alibaba Formation containing basalt, andesites and

pyroclastics. Average values of ^{40}K, ^{232}Th, ^{238}U, and dose rate in the Sarıçiçek granodiorite and surroundings were calculated as 2.98%, 12.45 ppm, 3.15 ppm, and 188.78 nGy/h, respectively.

Areas with high potassium concentration in the Sarıçiçek granodiorite were associated with granitic rocks that contain abundant rock forming minerals such as K-bearing feldspars (orthoclase, plagioclase). The quartz-bearing monzodiorites in the area contain K-poor minerals compared to other rocks [30]. Depending on this result, these low concentration areas were associated with quartz-bearing monzodiorites. While high values in the study area show that K is concentrated with eU and eTh, this increase in K concentration also indicates the presence of altered rocks in the environment.

Although high uranium values were obtained in the Sarıçiçek granodiorite, the highest concentration value was measured for andesitic rocks depending on the mineral content. When we examine the area in general, it can be said that eU, which has a rather irregular change as a result of surface weathering, shows an increasing trend from southwest to northeast. The areas where the eU concentration was low in the pluton can be explained by the transport of U to other places by factors such as surface waters or wind as a result of physical weathering. Areas of high concentration in the plutonic mass may be associated with light-colored rocks with a high content of quartz and therefore high SiO_2 content. In addition, the eTh concentration was measured at low values in some points on the mass, and this situation arises from magmatic rocks or soils that lost their acidic character as a result of weathering.

The eU/eTh ratio for the study area ranged from 0.031 to 1.034, with an average of 0.268. Although high values were observed in the margins and middle parts of the Sarıçiçek granodiorite, it was low in general in the mass. The Alibaba Formation had very high eU/eTh values. The eU/eTh ratio was 0.25 in continental crust [51] and 0.39 in the depleted upper mantle [52]. The eU/eTh values calculated for the study area showed that the rocks did not have completely crustal origin in the area but were a mixture of upper mantle and continental crust rocks. The sections with high eU/eTh ratio (0.4-1) are from the continental crust, and the areas with average values are from the mantle. The K/eU ratio varies in the range from 3280.9 to 53600 with a mean of 10303.21 for the whole area. The variation in K/eU ratios indicates that the melts from different mantle reservoirs were composed of various compositions in terms of source. Average K/eU values were given as 9475, 15607, 27245, and 12367 for the upper, middle, lower and total crusts, respectively [53]. Compared to the values defined in the study area, areas with the average K/eU ratio (10303.21) are very close to the values given for the upper crust. Therefore, they are associated with the continental upper crust. The calculated K/eTh ratio for all rock and soil samples in the study area ranged from 1121.95 to 8620.69 with an average of 2452.6. Areas with high K/eTh ratio in the Sarıçiçek granodiorite were associated with granites with high K content (Table 1).

To determine whether there was a relationship between the uranium, thorium, and potassium concentrations measured in the study area, the correlation coefficients between these radioelements were calculated and the results are presented in detail below. Graphs showing the relationships between K-eTh, K-eU, and eTh-eU for the Sarıçiçek granodiorite and its surroundings are given in Fig. 10. As a result of the evaluation, the correlation coefficient between K and eTh radioelements was calculated as 0.67, and there was a reliable and linear relationship between the two radioelements. However, since the geological formations in the area contain these radioelements (especially uranium) in different proportions between the K-eU (R^2=0.112) and eTh-eU (R^2=0.110) ratios, there is a lot of scattering in the graph and there was no relationship between them.

The eTh and K concentrations showed similar increases and decreases in both Sarıçiçek granodiorite and Alibaba Formation rocks (Fig. 9). The variation in eTh and K concentration maps is quite similar. However, the concentration changes in the eU map are independent of these two radionuclides. That is, at the points where eTh and K were high, uranium was low depending on the mineral content. Therefore, a linear relationship was observed between K and eTh in the relationship graphs (Fig. 10), while a dispersed distribution was observed in the graphs of K-eU and eTh-eU, originating from the irregular eU variation.

A potassium composite map was generated (Fig. 11a) combining K in red, K/eTh in green, and K/eU in blue. Three different colors of cyan, blue, red, and green represent different amounts of radionuclides on the K composite map. Despite the low K and eU content, the eTh content is high in the anomaly zones represented by green color in the middle parts of the Sarıçiçek granitoid. In basaltic rocks (blue areas), which are a member of the Alibaba Formation surrounding the granitoid mass, K and eTh are low, and uranium is somewhat higher. These areas, which are high in eTh and eU and low in K especially in the southeast of the study area, are represented by cyan color. The red-colored areas (low eU and eTh and high K) are associated with granitic rocks with high K content.

Table 1. The K, eTh, and eU concentrations and dose rate, ratios of the concentration, and the geochemical indicators of uranium remobilization in the Sarıçiçek granodiorite and surroundings

	K (%)	eTh (ppm)	eU (ppm)	D (nGy/h)	eU/eTh	eU/K	eTh/K	U_{me} (%)	F parameter	eU-(eTh/3,5)
Min.	0,8	0,5	2,9	30,435	0,031	0,186	1,16	-123,3	0,08	-3,98
Max.	5,22	8,9	23,6	153,12	1,034	3,047	8,91	62,36	2,92	6,357
Mean	2,98	3,15	12,45	87,54	0,268	1,09	4,20	-14,70	0,77	-0,402

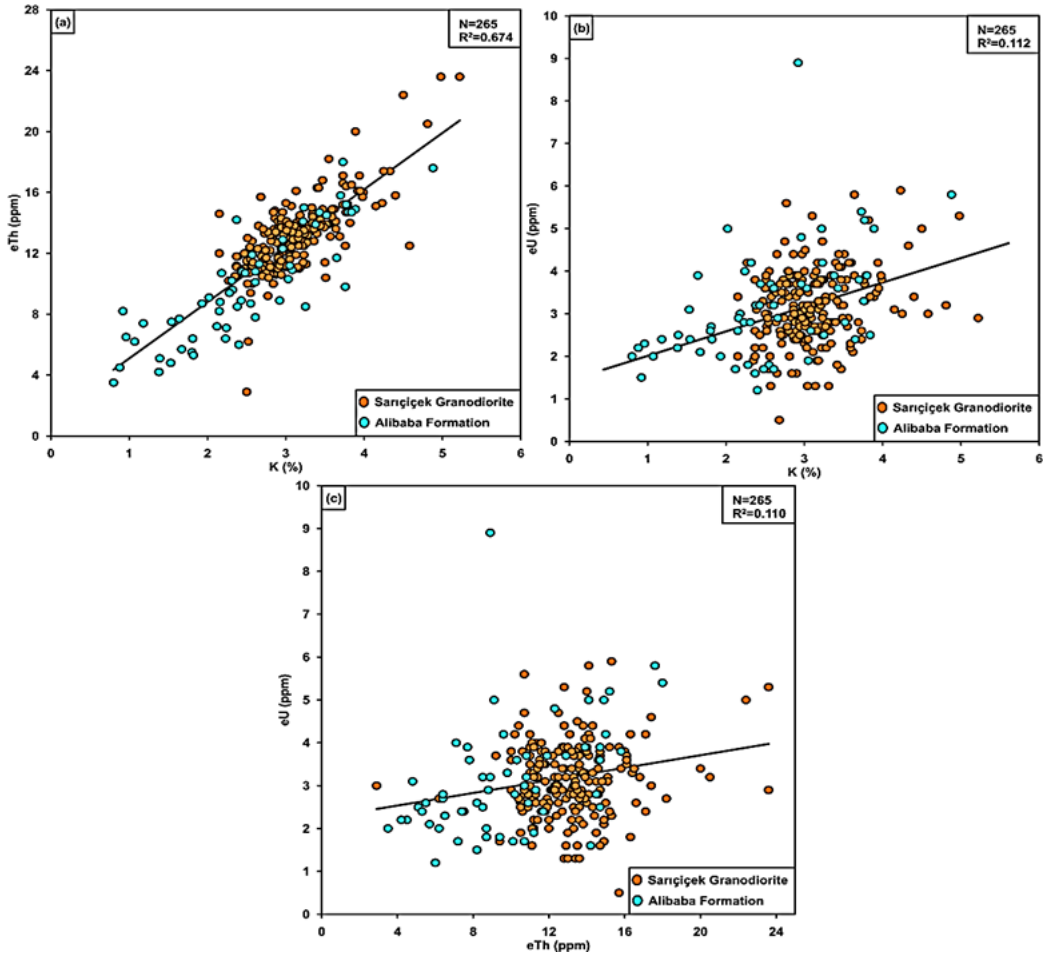

Figure 10. Variation diagrams of the Sarıçiçek granodiorite and surroundings: a) K vs eTh, b) K vs eU, and c) eTh vs eU modified from [15]

The eTh composite map is shown in Fig. 11b. Areas that are observed as large inclusions in the north, west, and south parts of the study area represented by blue reflect low K and eTh contents and high eU content, and these areas are associated with basaltic rocks. The high K and eTh values and low eU content in the granitoid mass are shown in yellow. The areas with low eTh with high K and eU contents appear as small scattered points in the study area and are represented by magenta color. These areas were interpreted as areas where soils and rocks with volcanic materials have lost their acidic properties as a result of weathering. The areas (bright green) with high eTh with low K and eU concentrations spread from west to east of the area and are associated with areas where the rocks are concentrated by remaining in the environment and thus contain this element.

When the eU composite map given in Fig. 11c is carefully examined, different colored anomaly zones which consist of inclusions of various sizes were observed throughout the study area. K and eTh have average values in the granitoid, especially where the eU content is very low, and these areas (represented by blue color) are associated with uranium-depleted granitic rocks. There are magenta-colored enclosures (high K and eU, and low eTh) observed in the granitoid mass. These highly concentrated areas are associated with rocks with high quartz content. Finally, the green areas indicate higher eTh concentration than eU and K contents in the rocks as a result of surface weathering in both the granitoid and the unit surrounding the granitoid. As can be seen from the composite map, uranium, which exhibits irregular change, shows an increasing trend from southwest to northeast.

The eU-(eTh)/3.5 ratio shows small changes towards the inner and marginal parts of the granodiorite (Fig. 12a). As with the eU concentration map, this rate of change has a distribution with high values especially in the marginal parts of the plutonic mass. For the study area, this ratio varies between -3.98 and 6.357, with an average value of -0.402. Negative values in the study area indicate uranium-poor areas, while positive values indicate uranium-rich areas. When the rate change in Fig. 9 and the eU map (Fig. 12a) are evaluated together, the eU concentration was quite low in areas showing negative values (the rate of change was very low), and this rate of change was positive, but rather high, in areas with high eU. Especially in the parts with negative values, this indicates that as the initial U content deteriorates, the radionuclide migrates.

In the mobility diagram (eU (ppm) versus eU-(eTh/3.5)) given in Fig. 12b, most of the data belonging to the Sarıçiçek granodiorite are below the zero line. In the Alibaba Formation, which consists of andesite, basalt, and pyroclasts surrounding the granodiorite, most of the data had positive values. The diagram clearly shows that there is uranium transport from the granodiorite to the Alibaba Formation and that these rocks are enriched with uranium.

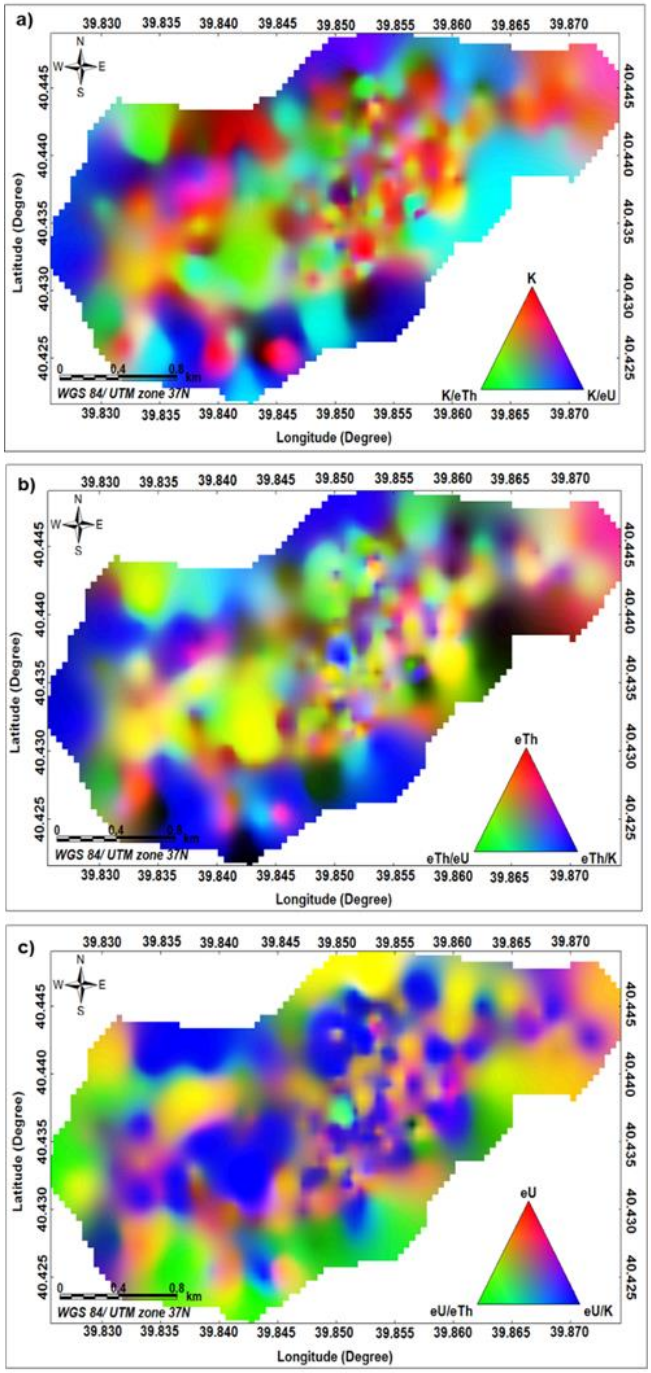

Figure 11. a) K, b) eTh, and c) eU composite image maps for the Sarıçiçek granodiorite and surroundings

The eU migration percentage calculated for Sarıçiçek granodiorite and surroundings ranges from -123.3 to 62.36, with an average of -14.70 (Fig. 12c, Table 1). Positive migration values obtained at the edges and northeast of the granodiorite in the study area indicate that migration is towards the inside of the unit. The fact that the migration percentage calculated for the Alibaba Formation is negative indicates that the U migration is outside the unit. Depending on some situations such as weathering, alteration, magmatic differentiation, sedimentation, and metamorphism, the uranium radionuclide in the environment moves from its environment to another environment, causing an increase and decrease. In the migration distribution map, there was uranium migration towards the surrounding rocks, especially in the NW of the study area.

The alteration parameter (F), which has a distribution very similar to the eU migration distribution map, was calculated to be high in Sarıçiçek granodiorite (Fig. 12d). This situation indicates that the eU and K concentrations in the granodiorite are high in places and accordingly there is a small amount of uranium enrichment in the area. While the average F parameter for the study area was calculated as 0.77, minimum and maximum values varied between 0.085 and 2.92.

On the ternary map (Fig. 13a), areas with low eU, K, and eTh concentrations are represented by black color and are associated with basalts in the Alibaba Formation. Small inclusions of with especially granite and andesitic rocks, in the northern and western parts of the study area are represented by white color, and these parts correspond to areas with high concentrations of all three radioelements. Areas of high eTh with low K and eU concentrations on the map are shown with green inclusions, while areas with low K and eTh but high eU concentrations in the northeastern and western parts of the study area are represented in blue. The red color corresponds to high K areas with low eU and eTh concentrations. There are magenta-colored enclosures (high K with low U and Th) observed that vary from place to place in the southern, southwestern, and northeastern parts of the study area area. Areas with high contents of K and eTh but low content of eU are characterized by yellow color.

A ternary diagram was plotted for the study area, with each axis representing a radioelement composition. When the measurements taken on the exposed rock and soils with volcanic composition were evaluated, the data were concentrated on the eTh axis in the triangular ternary diagram (Fig. 13b). This situation for the radioelement concentration in the study area varied depending on the lithological units and their mineral content.

4.2. Assessment of In-situ Gamma-ray Data in the Sarıhan Granodiorite and Surroundings

In the granodiorite, which has solid appearance, especially in the southern parts, the rocks are easily fragmented and look like soil due to arenization and hydrothermal weathering. Depending on this situation in Sarıhan granodiorite, changes have occurred in the contents of radioactive elements. When the concentration and dose rate maps created based on radioactivity measurements of the granodiorite and surrounding rocks are examined together, generally high and moderate inclusions were observed in the granodiorite mass for all three radionuclides (Fig. 14). The lowest concentration values were found in the Hozbirikyayla Formation (consisting of sandy limestones and limestone) and the ophiolitic olistostromal mélange containing sandstone, gravelly sandstone, basalt, and andesite. The highest radionuclide concentration and dose rate values were obtained in the Sarıhan granodiorite containing quartz diorite, granodiorite, and quartz monzodiorite [54].

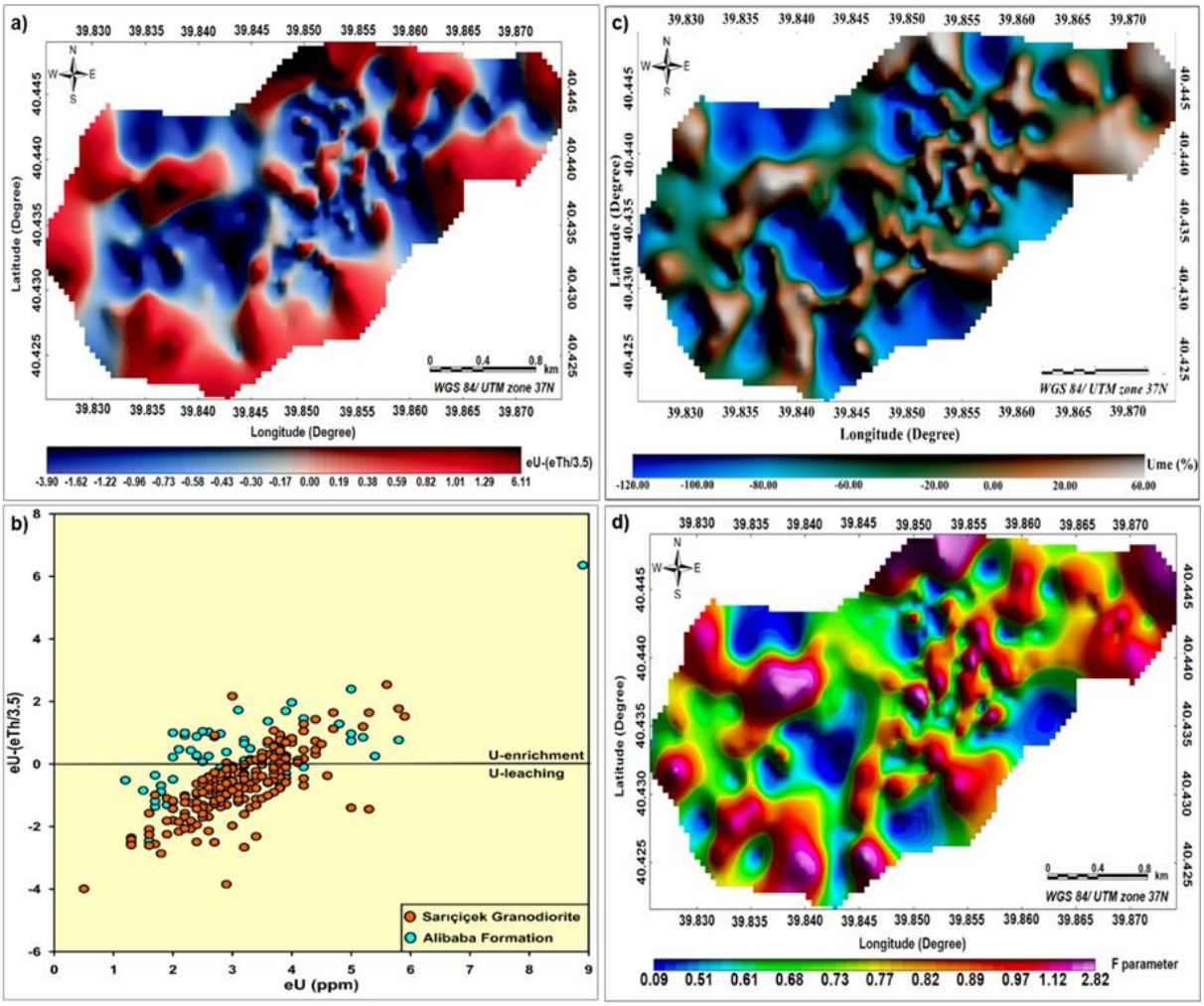

Figure 12. a) eU-(eTh/3.5) uranium mobility, b) eU (ppm) versus eU-(eTh/3.5) plot diagram, c) the uranium migration (U_{me} %), and d) F parameter maps for the Sarıçiçek granodiorite and surroundings

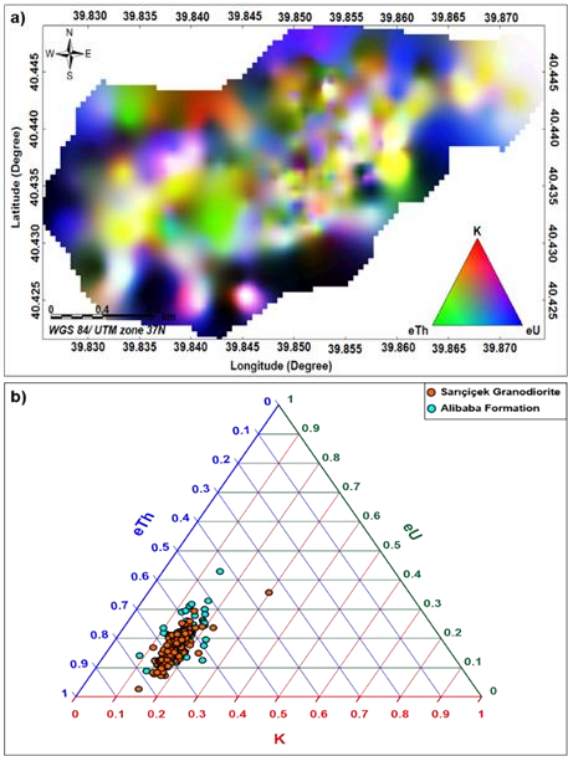

Figure 13. a) Radiometric ternary map, and b) eU–eTh–K ternary diagram for the study area

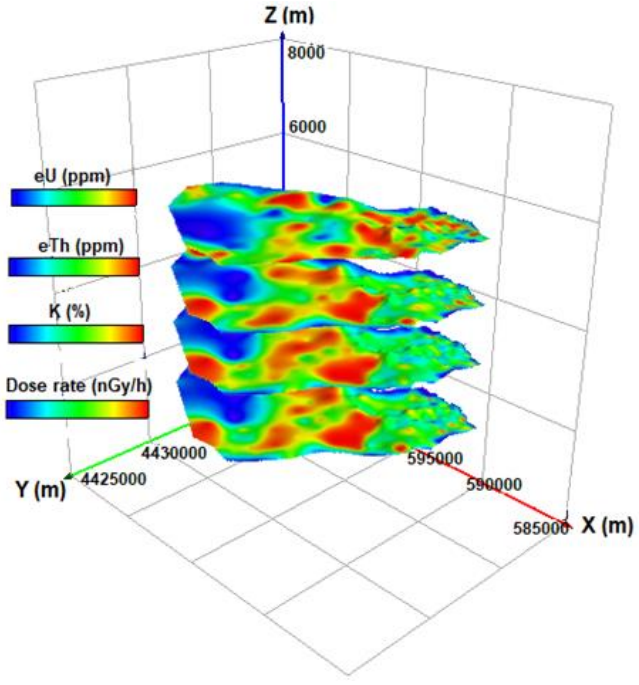

Figure 14. Three-dimensional representation of eU, eTh, K concentrations and dose rate distribution of Sarıhan granodiorite and its surroundings (Bayburt) modified from [15]

Potassium is abundant in rock-forming minerals, especially in K feldspars (orthoclase, microcline, and mica (biotite)). The plutonic rock contained 6-18% orthoclase and 1-85% biotite in the Sarıhan granodiorite [30]. Accordingly, areas with high K concentration were associated with rocks and soils containing these minerals. The reason why the potassium concentration was very low in the Hozbirikyayla Formation was concluded to be due to the carbonate content in the limestones forming this formation. The low concentration values measured in the study area can be explained by the precipitation of U in organic materials in rocks and soils, or by the transport of U minerals from the environment with the effect of factors such as surface waters or wind as a result of mechanical weathering in the rocks. The eU concentration distribution in the east of the study area was higher than in the west. This situation in the concentration distribution indicates that the element eU may have migrated from west to east.

eTh and K radionuclides were observed at high concentrations in the middle parts of the plutonic mass and places close to the ophiolitic mélange, while small areas with moderately high values were observed in the northeast. As with these two radionuclides, while the U radionuclide had high-value changes in the middle of the area, it also showed very high concentration changes, especially in the northeast of the study area. The areas where the dose rate and radionuclide concentrations are high were related to K feldspar and the pluton with abundant quartz and accordingly high SiO_2 content. Low radionuclide concentrations and dose rates were observed in the Hozbirikyayla Formation, which contains limestone and sandy limestone surrounding the Sarıhan granodiorite from the northwest to southeast.

According to the eU/eTh values given by researchers [51-52], the origin of the rocks in the study area was evaluated. The Sarıhan granodiorite and surrounding rocks were classified as continental crustal rocks according to average eU/eTh values. According to the eU/eTh ratio change calculated for the whole area, the rocks in the study area are a mixture of continental crust and depleted upper mantle. The low value (<0.3) region in the center of the study area corresponds to continental crustal rocks, while the values between 0.3-0.5 represent depleted upper mantle origin rocks. The places where the eU/eTh ratio is high corresponded to formation boundaries, especially where limestones are found.

The K/eU ratio for the study area varied between 62.5 and 33000 with an average of 7111.88. According to the K/eU ratio values [53], the average K/eU values for the study area were correlated with the continental upper crust. This ratio was calculated in previous studies [55]. In addition, the average K/eU ratio calculated for the area was also consistent with the K/U ratio (7000) values calculated in previous studies.

The average K/eTh ratio in the study area was 1376.15 and varied between 35.71 and 5000 (Table 2). Areas with a K/eTh ratio of 564.97-833.3 correspond to the mélange belt, while areas with a K/eTh ratio of 909.1 to 1428.57 correspond to Sarıhan granodiorite with high K content and areas with a high ratio (K/eTh=2500-5000) of limestones. The K/eTh ratio gives information about the structure of mica and feldspars, and the increase in this ratio is accepted as an indicator of the clay ratio.

Statistical evaluations were made for Sarıhan granodiorite and surroundings, as for the Sarıçiçek granodiorite, to determine correlations between radionuclide concentrations (K, eU, eTh). As seen in the correlation graphs (Fig. 15), although there was a good linear relationship (R^2=0.817) between K-eTh, there was almost no relationship between K-eU (R^2=0.234) and eTh-eU (R^2=0.158). Another reason why no relationship could be observed between the U radionuclide and these two radionuclides may be that the U radionuclide is highly affected by events such as surface weathering in the rocks and displays irregular changes depending on this situation. When the geological formations in the area are evaluated within themselves; while the Hozbirikyayla limestone showed the best K-eTh relationship, no relationship was observed between eTh and eU in the Sarıhan granodiorite.

As can be clearly seen from the composite maps prepared for each radionuclide, the color transitions in the map show good agreement with the geological formations in the study area. Radionuclide composite maps consist of the combination of the radionuclide in the rock or soil and the ratios of these radionuclides to each other, as shown in Fig. 16. As can be seen on the map, the equivalent uranium composite values vary according to the rock and soil type. While limestone is represented by green and yellow colors; blue, orange, and magenta colors are dominant within the granitoid. Blue areas on the map show areas associated with low K and eTh and high eU, while yellow represents low eU concentrations overlapping with sandy limestone in the southeast part of the area. There are magenta-colored areas (high K and eU and low eTh) varying from place to place from the southwest to the northeast of the study area (Fig. 16a).

On the map, which shows three distinct color changes of yellow, blue, and green, light colors are dominant especially on the granitoid, and the eTh content is relatively higher than eU and K in these areas. The equivalent thorium composite image map in Fig. 16b shows a blue area (high eU with low K and eTh) which has low content of eTh that coincides with the Hozbirikyayla Formation in the northwestern and southeastern parts of the study area. The areas represented by a dark color indicate rocks with low concentration values for eU, eTh, and K.

The potassium composite map created by using K radionuclide and K/eTh and K/eU ratios is given in Fig. 16c. As with the potassium concentration distribution map shown in Fig. 14, the areas represented by red color are associated with low equivalent thorium and equivalent uranium content versus high potassium content rocks. Potassium variation zones are shown as cyan-colored parts on the potassium composite image map, and these zones are related to rocks that have low K concentrations which coincide with limestones with high carbonate content.

Table 2. The K, eTh, and eU concentrations and dose rate, ratios of the concentration, and the geochemical indicators of uranium remobilization in the Sarıhan granodiorite and surroundings

	K (%)	eTh (ppm)	eU (ppm)	D (nGy/h)	eU/eTh	eU/K	eTh/K	U_{me} (%)	F parameter	eU-(eTh/3,5)
Min.	0,01	0,2	0,8	8,038	0,043	0,303	2	-160,47	0,06	-6,3
Max.	4,41	33,6	5,4	158,78	5,91	17,77	17,77	27,65	1,47	3,828
Mean	1,83	13,6	2,73	73,03	0,284	1,92	7,47	-48,44	0,38	-1,164

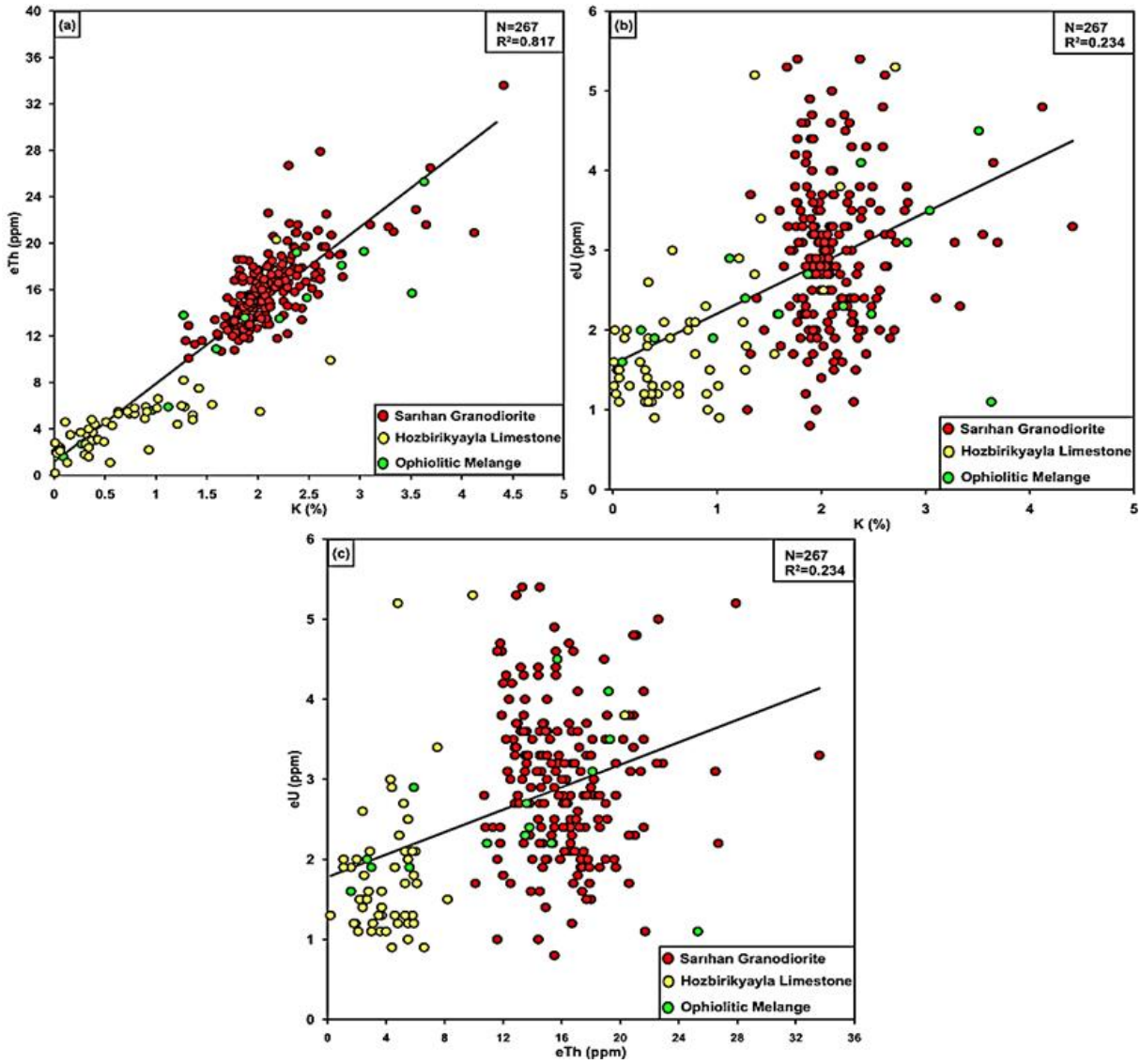

Figure 15. Variation diagrams of the Sarıhan granodiorite and surroundings: a) K vs eTh, b) K vs eU, and c) eTh vs eU modified from [15]

In the study area, high eU-(eTh)/3.5 values were obtained in the limestone and ophiolitic mélange, as with the other geochemical radionuclide ratios (Fig. 17a). While high and moderate values were observed in the northern part of the Sarıhan granodiorite, quite low values were obtained in the middle and southern parts of the plutonic mass. For the study area, this ratio varies between -6.3 and 3.828, with an average value of -1.164. This ratio also represents the original U content in the medium due to the remaining and immobile Th radionuclide. Over time, the U radionuclide, which is exposed to events such as decomposition and alteration in the formation, cannot maintain its original concentration and changes. The mobility diagram for the Sarıhan granodiorite and its surroundings is given in Fig. 17b. As with the Sarıçiçek granodiorite, most of the values in the granodiorite are negative values. Most values for the Hozbirikyayla limestone are above the zero line and there is uranium enrichment as a result of uranium transport from the granodiorite. There was a partial change in the values of the mélange belt, and increases and decreases were observed in the amount of uranium in the environment depending on the type of rock.

While the percentage of U migration calculated for the Sarıhan granodiorite and its surroundings had an average of -48.43, these values varied between -160.47 and 27.645 (Fig. 17c). Positive migration values obtained for the Sarıhan granodiorite in the study area show that the migration is towards the inside of the unit. The fact that the migration percentages calculated for the mélange and Hozbirikyayla Formation are negative

indicate that the U migration is outside the unit. While there is a decrease in the U concentration as a result of transport in the environment, it added to the existing U radionuclide in the environment where it was transported, causing an increase in the concentration.

The Efimov (F) parameter was calculated to be high for the Sarıhan granodiorite (Fig. 17d). This situation indicates that the eU and K concentrations in the granodiorite are high and accordingly there was U enrichment in the area. While the average F parameter for the entire study area was calculated as 0.381, minimum and maximum values ranged between 0.0057-1.473. Areas with high F values, as in Sarıçiçek granodiorite, indicate possible areas for metallic mines. The places where this parameter is high are associated with high-grade alteration zones and indicate areas with K enrichment related to the alteration of mafic minerals in the rocks during potassic alteration [56].

The ternary map for the Sarıhan granodiorite and surroundings is given in Fig. 18a. The dark areas represented by low values are related to limestone, and sandy limestones especially in the west to the northeast part of the Hozbirikyayla Formation surrounding the Sarıhan granodiorite and the eTh, K, and eU concentrations are low in these areas. The low uranium and high potassium and thorium parts on the map are shown in yellow, while the blue color in the southeast of the area corresponds to low uranium regions. Finally, light magenta color inclusions appearing in places coincide with low thorium and high uranium and potassium concentrations. In addition, areas identified by the light green color indicate uranium enrichment.

The ternary diagram is a diagram created base on certain constant equalization of the sum of three variable data sets, such as potassium, uranium, and thorium (Fig. 18b). This constant variable used in the definition is usually expressed as either 1.0 or 100%. In the study, it was assumed that the K, eU, and eTh variables are equal to 1.0. K, eU, and eTh concentrations measured in different lithological formations such as Sarıhan granodiorite, Hozbirikyayla Formation, and ophiolitic mélange belt are given on ternary diagram. According to the diagram, while the Sarıhan granodiorite exhibits high thorium values, the mélange belt and Hozbirikyayla formation have higher uranium values than this granitoid.

While the K_2O and SiO_2 contents of the rocks forming the non-adakitic Sarıçiçek granodiorite were between 2-4.5% and 58-75%, respectively [28], the K_2O and SiO_2 amounts for the adakitic Sarıhan granodiorite were between 2.16-2.76% and 61.16-65.29% [35]. According to the silica content, both Sarıçiçek granodiorite and Sarıhan granodiorite consist of rocks with a transitional composition (intermediate magma, between 53-65% Si) between felsic and mafic magma. These rocks with felsic magma composition rich in silica (Si) contain significant amounts of potassium, aluminum, and sodium and small amounts of magnesium, iron, and calcium. Adakitic rocks with high silica content and felsic magma composition are associated with high eTh/eU ratios due to low U and high Th content. This situation is explained by the transport and removal of elements such as U, Th, and Rb in the lower crust with the solution (especially the U radionuclide) during partial melting by many researchers [51].

In the study, the average eTh/eU ratio was calculated as 5.5 for the non-adakitic Sarıçiçek granodiorite and as 4.16 for the adakitic Sarıhan granodiorite [15]. The average eTh/eU ratios as a result of studies about adakitic rocks around the World were; Panamanian adakites [57] 2.7, Pulur adakites [37] 3.33, Kamchatka adakites [58] 2.8, Arkeen Wawa adakites [59] 4.5, and 3.4-6 in adakites found in volcanic zones in Chile [60]. The average eTh/eU value obtained for Sarıhan granodiorite with adakitic character in this study was closer to the mean crustal value (eTh/eU=4.0) [61], while adakitic rocks are generally represented with high eTh/eU values.

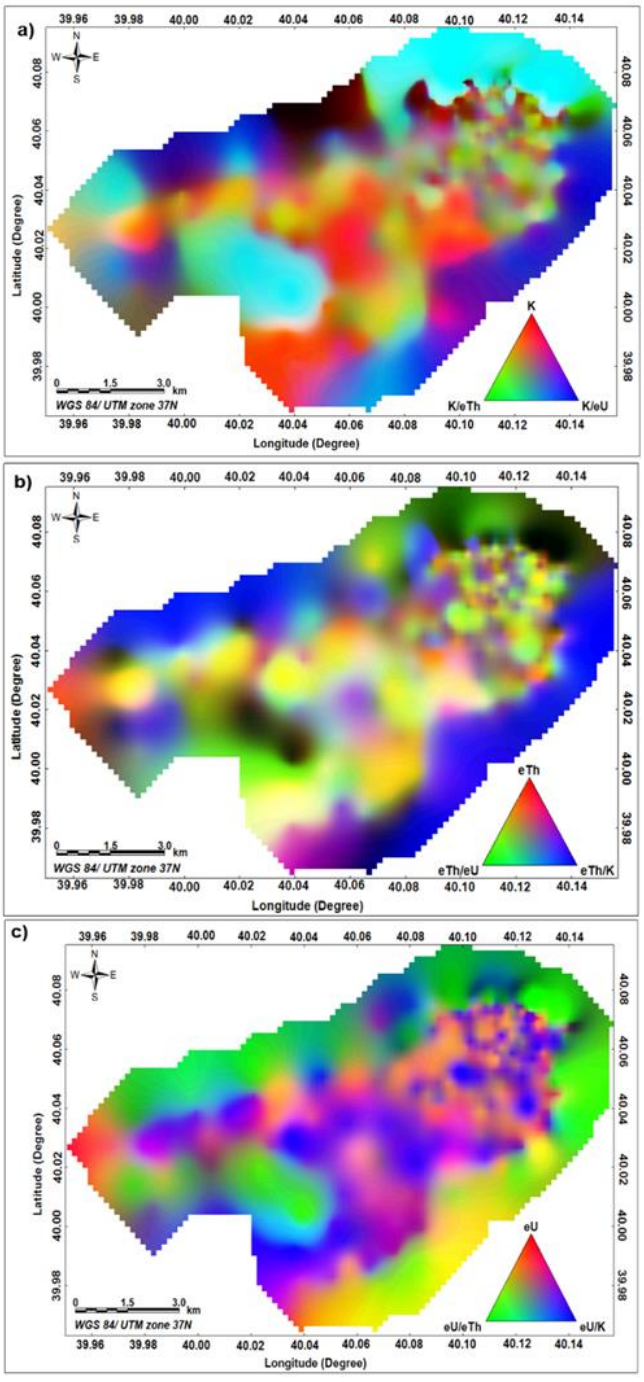

Figure 16. a) K, b) eTh, and c) eU composite image maps for the Sarıhan granodiorite and surroundings

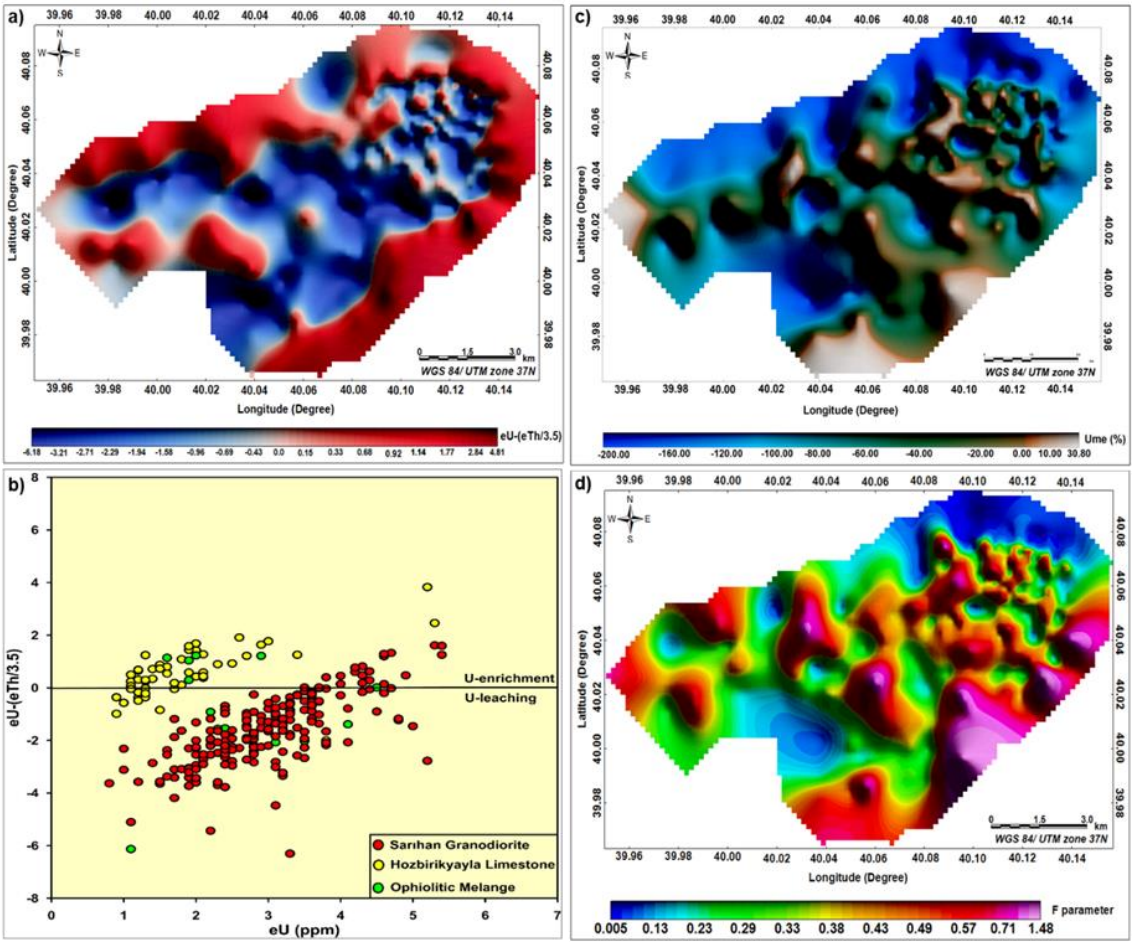

Figure 17. a) eU-(eTh/3.5) uranium mobility, b) eU (ppm) versus eU-(eTh/3.5) plot diagram, c) The uranium migration (U_{me} %), and d) F parameter maps for the Sarıhan granodiorite and surroundings

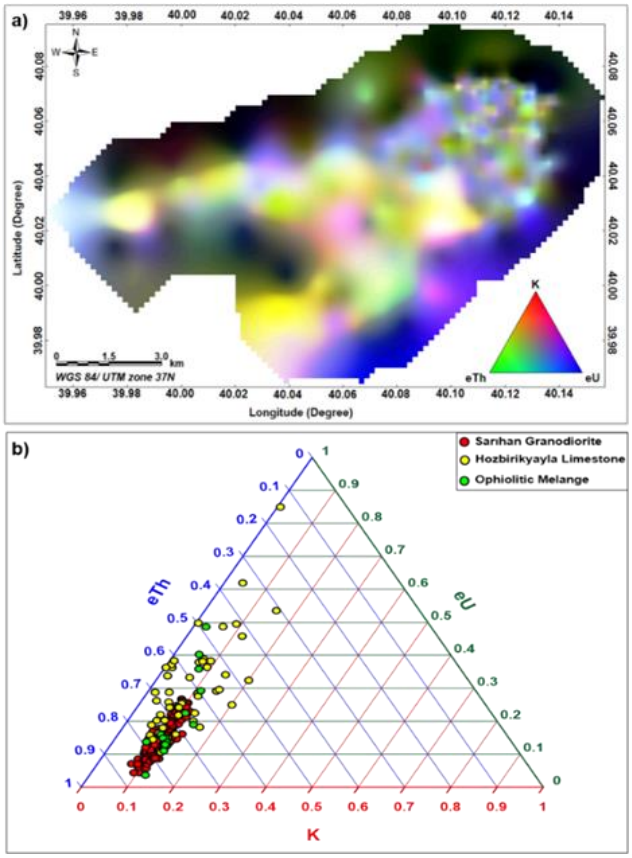

Figure 18. a) Radiometric ternary map, and b) eU–eTh–K ternary diagram for the study area

4.3 Laboratory Gamma Spectrometry Analysis of Samples Collected from Study Area (Gümüşhane)

The relationship between the data measured in the field and the data measured with the system with higher sensitivity in the laboratory was determined as activity unit (Bq/kg). The concentrations of K, eU, and eTh with in-situ measurements were recorded as % and ppm, respectively. Thus, in order to compare in-situ and laboratory measurements, concentration units must be converted into activity units [62]. The conversion factors for K, eU, and eTh in Bq/kg are 313, 12.35, and 4.06, respectively. The average activity concentrations of ^{232}Th, ^{238}U, and ^{40}K radioactive nuclei obtained from laboratory and field measurements (Table 3) for the samples analyzed are shown in Fig. 19. When Fig. 19 and Table 3 are examined together, low differences between the in situ and laboratory results were observed for the ^{238}U activity, while high differences were observed for the ^{40}K activity values.

The ranges of the activity concentrations of ^{238}U, ^{232}Th, and ^{40}K were 6.055-72.86 Bq/kg, 19.48-95.81 Bq/kg, and 287.96-1633.86 Bq/kg for the in-situ measurements, and 6.71-70.89 Bq/kg, 16.08-83.62 Bq/kg, and 208.72-1262 Bq/kg in the laboratory, respectively. The determined radionuclide activity concentrations were compared with studies in the literature for similar rock types [63-67]. As a result, no significant difference was found between in-situ and laboratory measurements.

Table 3. Average activity concentrations of ^{238}U, ^{232}Th and ^{40}K measured in laboratory and in-situ for Sarıçiçek granodiorite and its surroundings

Formation	Laboratory Measurements (HPGe detector)			In-situ Measurements (NaI(Tl) detector)		
	U (Bq/kg)	Th (Bq/kg)	K (Bq/kg)	U (Bq/kg)	Th (Bq/kg)	K (Bq/kg)
Alibaba Formation	29.2	37.05	422.436	35.72	45.12	543.71
Sarıçiçek Granodiorite	42.93	51.68	422.81	40.91	54.35	495.71

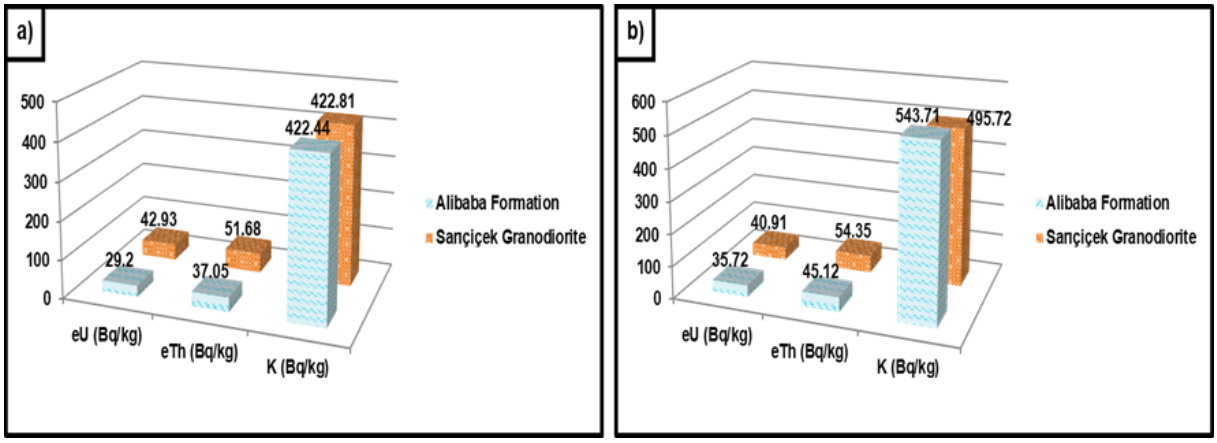

Figure 19. Activity concentrations of ^{232}Th, ^{238}U and ^{40}K obtained from a) HPGe (Laboratory) and b) NaI(Tl) (In-situ) detectors for Sarıçiçek granodiorite and surroundings modified from [15]

5. Conclusion

In this study, Sarıçiçek (Gümüşhane) and Sarıhan granodiorites (Bayburt) and their surrounding formations were examined by using portable spectrometry. The data measured and calculated in the field were represented on maps, which include maps of radionuclide concentrations, radionuclide ratios, composite image, and uranium remobilization maps.

In the radioactivity measurements carried out in the study areas, radionuclide concentrations showed irregular changes in both granodiorites due to the rock (consisting of quartz monzodiorite, granodiorite, and quartz diorite) and mineral differences (quartz, muscovite, sphene, biotite, and K-bearing feldspars (orthoclase, plagioclase)) in the formations. While the highest radionuclide concentrations (eU, eTh, and K) were mostly observed in granodioritic masses, low values were obtained in the formations surrounding these masses. Based on the average eU/eTh, K/eTh, and K/eU data, the rocks in the study area do not entirely have crustal origin, but formed as a result of a mixture of upper mantle and continental crust. It was concluded that the irregular changes in the main, trace, and rare earth elements in the rocks were affected by differentiation during crystallization to a high degree, partial melting events to a partial degree, and also hybridization of two magmas during the formation of the rocks. These results are supported by the results obtained in other studies [40,28].

When the study is evaluated in terms of uranium mobility, positive migration values obtained for the Sarıçiçek and Sarıhan granodiorites show that the migration is towards the inside of the unit, while the negative values for the surrounding formations indicate that the U migration was outside the units. To summarize uranium migration or transport in the study, uranium transport was not related to chemical weathering but to the transportation of rock fragments and soil as a result of physical weathering (wind, surface waters, tectonic, etc.) and the accumulation of radionuclides in these units.

There are differences between the data measured in two different environments, as can be seen from the data obtained from the in-situ and laboratory measurements. This may be caused by factors related to the device used for measurement (crystal difference in the detector, crystal volume, calibration) and the measurement time, or external factors (cosmic rays, radioisotope particles in the air, soil humidity, vegetation, etc.) in the area where the measurement is made. During in-situ measurement with a gamma-ray spectrometer, the value measured in each window of the spectrometer; that is, the number of gamma rays is equal to the sum of the gamma rays coming from terrestrial and extraterrestrial sources. As a result of this situation, the *in-situ* results obtained in this study were higher than the laboratory results for ^{238}U, ^{232}Th, and ^{40}K. In brief, there was no significant difference between the results of the in situ measurements with the NaI(Tl) detector and the laboratory analysis made with the HPGe detector for the activity values.

To summarize briefly, nowadays, chemical and petrological variations in rocks can be investigated and mapped quickly and easily, depending on the relationship between geology and radionuclide concentrations, especially in areas where granitic rocks are present, with in situ gamma-ray spectrometry measurements (K, U, and Th concentrations).

Acknowledgement

We would bluntly like to express our gratitude to the reviewers and the editor of the Journal, for their helpful criticism and detailed discussions and suggestions that improved the manuscript. Grateful thanks are offered to the provider of financial support for the research presented here: Karadeniz Technical University

Scientific Research Project (Project no: BTAP-9588). A part of this study was presented as an oral presentation at the congress named International Online Conferences on Engineering and Natural Sciences (IOCENS 2021).

Author contributions

Suna Altundaş: Conceptualization, Methodology, Software Interpretation, Visualization, Writing-Original draft preparation, Field study. **Hakan Çınar:** Investigation, Writing-Reviewing and Editing.

Conflicts of interest

The authors declare that they have no known competing financial interests or personal relationships that could have appeared to influence the work reported in this paper.

References

1. Dizman, S. (2006). Measurement of natural radioactivity level in Rize-centre and towns of Rize. Master thesis, Karadeniz Technical University, Graduate School of Natural and Applied Sciences, Trabzon, Turkey.
2. Valkovic, V. (1984). Radioactivity in the Environment. Elsevier Science B. V., Netherlands.
3. Kathren, R.L. (1984). Radioactivity in the Environment: Sources, Distribution and Surveillance. Harwood Academic Publishers, New York.
4. UNSCEAR. (2000). United Nations Sources and Effects of Ionizing Radiation. Volume I: Sources; Volume II: Effects. United Nations Scientific Committee on the Effects of Atomic Radiation, Report to the General Assembly, with scientific annexes. United Nations sales publications E.00.IX.3 and E.00.IX.4. United Nations, New York.
5. Apaydın, G., Köksal, O.K., Cengiz, E., & Tıraşoğlu, E., Baltas, H., Karabulut, K., & Söğüt, Ö. (2019). Assessment of natural radioactivity and radiological risk of sediment samples in Karacaören II dam Lake, Isparta/Turkey. ALKÜ Fen Bilimleri Dergisi, 28-35.
6. Canbaz, B., Çam, N.F., Yaprak, G., & Candan, O. (2010). Natural radioactivity (^{226}Ra, ^{232}Th and ^{40}K) and assessment of radiological hazards in the Kestanbol granitoid, Turkey. Radiation Protection Dosimetry, 141,192-198.
7. Tzortzis, M., Tsertos, H., Christofides, S., & Christodoulides, G. (2003). Gamma-ray measurements of naturally occurring radioactive samples from Cyprus characteristic geological rocks. Radiation Measurements, 37, 221–229.
8. Naumov, G.B. (1959). Transportation of uranium in hydrothermal solution as a carbonate. Geochemistry, 1, 5-20.
9. Aydın, İ. (2004). Radiometric method and Gamma-ray spectrometer in Geophysics.
10. Abd El-Mageed, I.A., El-Kamel, H.A., & Abbady, A. (2011). Assessment of natural and anthropogenic radioactivity levels in rocks and soils in the environments of Juban town in Yemen. Radiation Physics and Chemistry, 80, 710–715.
11. Heikal, M.Th.S., El-Dosuky, B.T., Ghoneim, M.F., & Sherif, M.I. (2012). Natural radioactivity in basement rocks and stream sediments, Sharm El Sheikh Area, South Sinai, Egypt: Radiometric levels and their significant contributions. Arabian Journal of Geosciences.
12. Youssef, A., Hassan, A., & Mohamed, M. (2009). Integration of remote sensing data with the field and laboratory investigation for lithological mapping of granitic phases: Kadabora pluton, Eastern Desert, Egypt. Arabian Journal of Geosciences, 2, 69-82. https://doi.org/10.1007/s12517-008-0020-2.
13. Azzaz, S., Arnous, M., Elmowafy, A., Salem Kamar, M., Abdel Hafeez, W. (2018). Lithological discrimination and mapping using digital image processing, petrographic and radioactive investigation of Wadi Dahab area, Southeastern Sinai, Egypt. Middle East Journal of Applied Sciences, 8, 444-464.
14. Bayoumi, M.B., & Emad, B.M. (2020). Mapping and Lithological discrimination using digital image processing and radioactive investigations of Wadi Um Gheig area, Central Eastern Desert, Egypt. Middle East Journal of Applied Sciences, 10, 737-754. https://doi.org/10.36632/mejas/2020.10.4.65.
15. Altundas, S. (2016). Investigation of Sarıçiçek and Sarıhan Granodiorites using in-situ Gamma-Ray Spectrometer and Magnetic Susceptibility Methods. PhD thesis (in Turkish with an English abstract), Karadeniz Technical University, Trabzon.
16. Pourimani, R., Zare, M.R., & Ghahri, R. (2014). Natural radioactivity concentrations in Alvand granitic rocks in Hamadan, Iran. Radiation Protection and Environment, 37, 132-140. https://doi.org/10.4103/0972-0464.154866.
17. Papadopoulos, A., Altunkaynak, S., Koroneos, A., Ünal, A., & Kamacı, Ö. (2016). Distribution of natural radioactivity and assessment of radioactive dose of Western Anatolian plutons, Turkey. Turkish Journal of Earth Sciences, 25, 434-455. https://doi.org/ 10.3906/yer-1605-4.
18. Maden, N., Akaryalı, E., & Çelik, N. (2019). The in situ natural radionuclide (238U, 232Th and 40K) concentrations in Gümüşhane granitoids: implications for radiological hazard levels of Gümüşhane city, northeast Turkey. Environmental Earth Sciences, 78, 330. https://doi.org/10.1007/s12665-019-8333-x.
19. Yalcin, F., Ilbeyli, N., Demirbilek, M., Yalcin, M.G., Gunes, A., Kaygusuz, A., & Ozmen, S.F. (2020). Estimation of Natural Radionuclides' Concentration of the Plutonic Rocks in the Sakarya Zone, Turkey Using Multivariate Statistical Methods. Symmetry, 12, 1048. https://doi.org/10.3390/sym12061048.
20. Saleh, G.M., Kamar, M.S., Rashed, M.A., & El-Sherif, A.M. (2015). Uranium Mineralization and Spectrometric Prospecting along Trenches of Um Safi area, Central Eastern Desert of Egypt. Geoinformatics & Geostatistics: An Overview, 3, 1. https://doi.org/10.4172/2327-4581.1000128.
21. Awad, H.A., Zakaly, H.M.H., Nastavkin, A.V., El-Tohamy, A.M., & El-Taher, A. (2021). Radioactive

mineralization on granitic rocks and silica veins on shear zone of El-Missikat area, Central Eastern Desert Egypt. Appl. Radiation Isotopes, 168. https://doi.org/10.1016/j.apradiso.2020.109493.
22. Hassan, S.M., Youssef, M.A.S., Gabr, S.S., & Sadek , M.F. (2022). Radioactive mineralization detection using remote sensing and airborne gamma-ray spectrometry at Wadi Al Miyah area, Central Eastern Desert, Egypt. The Egyptian Journal of Remote Sensing and Space Science, 25, 37-53. https://doi.org/10.1016/j.ejrs.2021.12.004.
23. Attia, T.E., & Shendi, E.H. (2013). Uranium migration history inthe igneous and metamorphic rocks of Solaf-Umm Takha area, based on multi-variate statistical analysis and favorability indices, central south Sinai, Egypt. IOSR Journal of Applied Geology and Geophysics (IOSR-JAGG), 1, 9-20. https://doi.org/10.13140/2.1.1438.9444.
24. Dessouky, O., & Ali, H. (2018). Using Portable Gamma-Ray Spectrometry for Testing Uranium Migration: A Case Study from the Wadi El Kareim Alkaline Volcanics, Central Eastern Desert, Egypt. Acta Geologica Sinica, 92, 2214-2232. https://doi.org/10.1111/1755-6724.13724.
25. Sundararajan, N., Pracejus, B., Al Khirbash, S., Al Hosni, T., Ebrahimi, A., Al-lazki, A., & Al-Mushani, M. (2019). Radiometric Surveys for Detection of Uranium in Dhofar Region, Sultanate of Oman. Sultan Qaboos University Journal for Science [SQUJS], 24, 36-46. https://doi.org/10.24200/squjs.vol24iss1pp36-46.
26. Khattab, M.R., Tawfic, A.F., & Omar, A.M. (2021). Uranium-series disequilibrium as a tool for tracing uranium accumulation zone in altered granite rocks, International Journal of Environmental Analytical Chemistry, 101(12), 1750-1760. https://doi.org/10.1080/03067319.2019.1686495.
27. Akingboye, A.S., Ademila, O., Okpoli, C.C., Oyeshomo,7A.V., Ijaleye, R.O., Faruwa, A.R., Adeola, A.O., & Bery, A.A. (2022). Radiogeochemistry, uranium migration, and radiogenic heat of the granite gneisses in parts of the southwestern Basement Complex of Nigeria. Journal of African Earth Sciences, 188. https://doi.org/10.1016/j.jafrearsci.2022.104469.
28. Karslı, O. (2002). Petrographic, mineralogical and chemical findings for magma interactions in granitoid rocks: Dölek and Sarıçiçek plutons (Gümüşhane, NE-Turkey). PhD Thesis, Karadeniz Technical University, Institute of Science, Trabzon.
29. Aydın, A., Ferre, E.C., & Aslan, Z. (2007). The Magnetic Susceptibility of Granitic Rocks as a Proxy for Geochemical Composition: Example from the Saruhan Granitoids, NE Turkey. Tectonophysics, 441, 85-95.
30. Aslan, Z. (2005). Petrography and Petrology of the Calc-Alkaline Sarıhan Granitoid (NE Turkey): An Example of Magma Mingling and Mixing. Turkish Journal of Earth Sciences, 14, 185-207.
31. Ketin, İ. (1966). Tectonic Units of Anatolia. Journal of MTA, 66, 20-43.
32. Bektaş, O., Yılmaz, C., Taslı, K., Akdağ, K., & Özgür, S. (1995). Cretaceous rifting of the eastern Pontide carbonate platform (NE Turkey): the formation of carbonates breccias and turbidites as evidences of a drowned platform. Geologia, 57(1-2), 233-244.
33. Bektaş, O., Şen, C., Atıcı, Y., & Köprübaşı, N. (1999). Migration of the Upper Cretaceous subduction-related volcanism toward the back-arc basin of the eastern Pontide magmatic arc (NE Turkey). Geological Journal, 34, 95-106.
34. Eyüboğlu, Y., Dudas, F.O., Santosh, M., Xiao, Y., Yi, K., Chatterjee, N., Wu, F.Y., & Bektaş, O. (2016b). Where are the remnants of a Jurassic Ocean in the Eastern Mediterranean Region. Gondwana Research, 33, 63-91. https://doi.org/10.1016/j.gr.2015.08.017.
35. Eyüboğlu, Y., Chung, S.L., Santosh, M., Dudasi, F.O., & Akaryali, E. (2011). Transition from shoshonitic to adakitic magmatism in the eastern Pontides, NE Turkey: implications for slab window melting. Gondwana Res., 19, 413-429.
36. Karslı, O., Chen, B., Aydın, F., & Şen, C. (2007). Geochemical and Sr-Nd-Pb isotopic compositions of the Eocene Dölek and Sarıçiçek Plutons, Eastern Turkey: implications for magma interaction in the genesis of high-K calc-alkaline granitoids in a post-collision extensional setting. Lithos, 98, 67-96.
37. Eyüboğlu, Y., Santosh, M., Dudas, F.O., Akaryali, E., Chung, S.L., Akdag, K., & Bektas, O. (2013a). The nature of transition from adakitic to non-adakitic magmatism in a slab-window setting: A synthesis from the eastern Pontides, NE Turkey. Geoscience Frontiers, 4, 353-375.
38. Güven, İ.H. (1993). Geological and metallogenic map of the Eastern Black Sea Region, 1:250000 Map, MTA, Trabzon.
39. Eyüboğlu, Y., Chung, S.L., Dudas, F.O., Santosh, M., Akaryali, E. (2011). Transition from shoshonitic to adakitic magmatism in the Eastern Pontides, NE Turkey: Implications for slab window melting. Gondwana Research, 19, 413-429.
40. Aslan, Z. (1998). Petrography, Geochemistry and Petrology of Saraycık-Sarıhan Granitoid (Bayburt) and Surrounding Rocks and Geocronology of Sanhan Granitoid. PhD thesis, Karadeniz Technical University, Trabzon.
41. IAEA. (1974). Instrumentation for uranium and thorium exploration, International Atomic Energy Agency Technical reports series No. 158, Vienna.
42. Killeen, P.G., & Cameron, G.W. (1977). Computation of in situ potassium, uranium and thorium concentrations from portable gamma-ray spectrometer data. In: Report of activities, part A, Geological Survey of Canada, 77-1A, 91–92.
43. GF Instruments. (2009). Gamma Surveyor User Manual. GF-Instruments: Brno, Czech Republic.
44. Darnley, A.G. (1973). Airborne Gamma-Ray Techniques-Present and Future; Uranium Exploration Methods. International Atomic Energy Agency, Proceedings of a Panel, Vienna, 67-108.
45. Boyle, R.W. (1982). Geochemical prospecting for thorium and uranium deposits. Development Economic Geology 16, Elsevier, Amsterdam.
46. Clark, S.P., Peterman, Z.E., & Heier, K.S. (1966). Abundance of U, Th and K. In Handbook of Physical constants. Geology Society of America, 97, 521-541.

47. NMA. (1999). A report of work progression during II sub-stage (December, 1998-February, 1999) on uranium evaluation in Abu-Zeneima Area, Sinai, Egypt. Confidential Report, NMA, Cairo, Egypt.
48. Youssef, M.A.S., Sabra, M.A.M., Abdeldayem, A.L., Masoud, A.A., & Mansour, S.A. (2017). Uranium migration and favourable sites of potential radioelement concentrations in Gabal Umm Hammad area, Central Eastern Desert, Egypt. NRIAG Journal of Astronomy and Geophysics, 6, 368–378.
49. Efimov, A.V. (1978). Multiplikativniyj pokazatel dlja vydelenija endogennych rud aerogamma-spectrometriceskim dannym, in Metody rud-noj geofiziki: Lenigrad, Naucnoproizvods-tvennoje objedinenie. Geofizica Ed., 59–68.
50. Asfahani, J., Aissa, M., & Al-Hent, R. (2010a). Aerial Spectrometric Survey for Localization of Favorable Structures for Uranium Occurrences in Al-Awabed Area and its Surrounding (Area-3), Northern Palmyrides–Syria. Applied Radiation and Isotopes, 68, 219-228.
51. Rudnick, R.L., & Fountain, D.M. (1995). Nature and composition of the continental crust: A lower crustal perspective. Reviews of Geophysics, 33, 267-309.
52. Sun, S.S., & McDonough, W.F. (1989). Chemical and isotopic systematics of oceanic basalts: implications for mantle composition and processes. In: Saunders AD, Norry MJ (Eds.), Magmatism in the Oceanic Basins. Geological Society of London Special Publication, 42, 313–345.
53. Taylor, S.R., & McLennan, S.M. (1985). The Continental Crust: Its Composition and Evolution. Blackwell, Oxford.
54. Çınar, H., Altundaş, S., Çelik, N., & Maden, N. (2017). In situ gamma ray measurements for deciphering of radioactivity level in Sarıhan pluton area of northeastern Turkey. Arabian Journal of Geosciences, 10(19). https://doi.org/ 10.1007/s12517-017-3225-4.
55. Davies, G.F. (1999). Geophysically constrained mantle mass flows and the ^{40}Ar budget: a degassed lower mantle. Earth Planet. Sci. Lett., 166, 149–162.
56. Akaryalı, E., (2010). Geological, mineralogical, geochemical and genetic investigation of the Arzular (Gümüshane Northeast-Turkey) gold deposit, Ph.D. Thesis, Karadeniz Technical University, Institute of Science and Technology, Trabzon.
57. Defant, M.J., Jackson, T.E., Drummond, M.S., De Boer, J.Z., Bellon, H., Feigenson, M.D., Maury, R.C., & Stewart, R.H. (1992). The geochemistry of young volcanism throughout western Panama and southeastern Costa Rica: an overview. J. Geol. Soc. (Lond.), 149, 569-579.
58. Kepezhinskas, P., McDermott, F., Defant, M., Hochstaedter, A., Drummond, M.S., Hawkesworth, C.J., Koloskov, A., Maury, R.C., & Bellon, H. (1997). Trace element and Sr–Nd–Pb isotopic constraints on a three component model of Kamchatka arc petrogenesis. Geochim. Cosmochim. Acta, 60, 1217-1229.
59. Polat, A., & Kerrich, R. (2001). Magnesian andesites, Nb-enriched basalts and adakites from late-Archaean 2.7 Ga Wawa greenstone belts, superior Province, Canada. Implications for late Archaean subduction zone petrogenetic processes. Contrib. Mineral. Petrol., 2141, 36-52.
60. Sigmarsson, O., Martin, H., & Knowles, J. (1998). Melting of subducting oceanic crust from U–Th disequilibria in austral Andean lavas. Nature, 394, 566–569.
61. Galer, S.J.G., & O'Nions, R.K. (1985). Residence time for thorium, uranium and lead in the mantle with implications for mantle convection. Nature, 316, 778–782.
62. IAEA. (1989). Construction and use of calibration facilities for radiometric field equipment. In: Proceedings of IAEA technical reports series 309, International Atomic Energy Agency, Vienna.
63. Dżaluk, A., Malczewski, D., Żaba, J., & Dziurowicz, M. (2018). Natural radioactivity in granites and gneisses of the Opava Mountains (Poland): a comparison between laboratory and in situ measurements. J. Radioanal Nucl. Chem. 316, 101–109.
64. Hassan, N.M., Kim, Y.J., Jang, J., Chang, B.U. & Chae, J.S. (2018). Comparative study of precise measurements of natural radionuclides and radiation dose using in-situ and laboratory γ-ray spectroscopy techniques. Sci. Rep. 8, 14115.
65. Kranrod, C., Chanyotha, S., Pengvanich, P., Kritsananuwat, R., Ploykrathok, T., Sriploy, P., Hosoda, M., & Tokonami, S. Comparative study of natural radionuclides measurements and radiation dose assessment using vehicle-borne and laboratory gamma-ray spectroscopy techniques in Thailand.
66. Al-Masri, M.S., & Doubal, A.W. (2013). Validation of in-situ and laboratory gamma spectrometry measurements for determination of ^{226}Ra, ^{40}K and ^{137}Cs in soil. Applied Radiation and Isotopes, 75, 50-57.
67. Arogunjo, A.M., Farai, I.P., & Jibiri, N.N. (2002). Comparison of in situ and laboratory gamma-ray spectroscopy of terrestrial gamma radiation in Ibadan, South Western Nigeria. Global Journal of Pure and Applied Sciences, 8, 505-509.